Compartmentation of the β-adrenergic signal by phosphodiesterases in adult rat ventricular myocytes

by

Jesse Milo Schwartz

A thesis submitted to the Department of Physiology

In conformity with the requirements for

the degree of Master of Science

Queen's University

Kingston, Ontario, Canada

(January, 2008)

ABSTRACT

Previous studies have suggested that phosphodiesterase (PDE) hydrolysis of cyclic adenosine monophosphate (cAMP) is important in the generation of specific and segregated cAMP signals within cells. The purpose of this study was to determine if PDE compartmentation was important in cardiac ventricular myocytes. Therefore, we investigated the effects of β-adrenergic (β-AD) stimulation with isoproterenol in the presence of cilostamide, a PDE3 inhibitor, or Ro 20-1724, a PDE4 inhibitor, on unloaded cell shortening, L-type calcium currents and intracellular calcium levels in freshly dissociated adult rat ventricular myocytes. PDE3 inhibition resulted in a 216 ± 17 % (n=8) increase in unloaded cell shortening after ten minutes of isoproterenol exposure, whereas isoproterenol produced a statistically smaller increase of 155 ± 12 % (n=8) in the presence of PDE4 inhibition. There was a non-significant trend for PDE4 inhibition to produce larger increases in calcium currents (179 ± 17 % (n=4) of controls) than PDE3 inhibition (155 ± 10 % (n=6) of controls). Both PDE3 and PDE4 inhibitors had similar effects on isoproterenol-stimulated increases of calcium transient amplitude with values of 209 ± 14 % (n=8) and 185 ± 12 % (n=8), respectively. Determination of sarcoplasmic reticulum (SR) calcium load using caffeine pulse experiments demonstrated that PDE4 inhibition and isoproterenol superfusion produced a statistically larger increase in SR-calcium loading (139 ± 9 % (n=6)) than PDE3 inhibition and isoproterenol superfusion (113 ± 9 % (n=6)). These results suggest that PDE3 may be active in proximity to the contractile apparatus of cardiac myocytes, whereas PDE4 may be localized in a domain consisting of the L-type calcium channel and junctional SR. Consequently, our study

provides functional evidence for differential localization of PDE isoforms in cardiac myocytes.

ACKNOWLEDGEMENTS

I would like to start by thanking my family. Thank you Noa, for encouraging me to "do the work," Sheldon, for giving me a good brain, and Jacob, for being my friend and exchanging funny stories on the phone. I would also like to thank my grandmother, Anne. You're one of the few grandmothers I can imagine who would take such an active interest in my research, and combine it with a capacity to really understand what I do.

I would like to acknowledge my housemates Gursev and Adrian. It is only in retrospect that I appreciate how lucky I was to live with you. A special thanks to Gursev for helping me with so many things and for all your sage advice, your friendship means a great deal to me.

I would like to thank the members of the Ward lab. Thank you Gina, for being there with me from the beginning, and Clarissa, for your assistance with prep work. A special thanks to Jimmy and Lian. Jimmy, you made working in the lab a lot of fun. Lian, you came to the rescue at exactly the right time. You're an excellent student and I know you will be successful. I would also like to thank the Ward lab volunteers, Dr. Melo, and all my friends and colleagues in the Melo lab.

Thank you Chris, for all your help and encouragement over the past two years. I learned a tremendous amount by working in your lab that will stay with me for the rest of my life. If I could go back and do it again, I wouldn't do my Master's anywhere else.

I would like to acknowledge the rats I used to acquire the data for my Master's. I will strive to take the knowledge I have gained from this experience and use it to benefit others.

My Master's is dedicated to the memory of my grandfather, Joshua Heilman.

TABLE OF CONTENTS

LIST OF TABLES

LIST OF FIGURES

LIST OF ABBREVIATIONS

AC……..adenylyl cyclase

AKAP…… A-kinase anchoring protein

β-AD…….. β-adrenergic

β-AR……...β-adrenergic receptors

CaM kinase…… Ca^{2+}/calmodulin dependent kinase

cAMP……cyclic adenosine monophosphate

Cav-3……..Caveolin-3

cGMP……cyclic guanosine monophosphate

CICR…….……calcium-induced calcium release

CNG……...cyclic nucleotide-gated

COPD……chronic obstructive pulmonary disease

CPVT……catecholaminergic polymorphic ventricular tachycardia

DAD……. delayed after-depolarization

DAG…….. diacylglycerol

ECC……excitation contraction coupling

EHNA…… erythro-9-(2-hydroxy-3-nonyl)adenine

eNOS……..endothelial nitric oxide synthase

EP……E-prostanoid

F……fluorescence intensity

F_0……basal fluorescence intensity

FKBP12.6…….. Calstabin 2

FRET……..fluorescence resonance energy transfer

FSK…… forskolin

GC……..guanylyl cyclase

GPCR……... G-protein coupled receptor

HCN2…… hyperpolarization activated cyclic nucleotide-gated cation channel

IBMX…… 3-isobutyl-1-methylxanthine

$I_{Ca,L}$…… L-type calcium channel

I_{K1}…….. inward rectifier potassium current

I_{NCX}…… sodium-calcium exchange current

IP_3…….. inositol-1,4,5-trisphosphate

I_{sus}…….. delayed rectifier potassium current

I_{to}…… transient outward potassium current

LZ…….. leucine zipper

mAKAP…… muscle A-kinase anchoring protein

MBCD……methyl-beta cyclodextrin

MI…….. myocardial infarction

NO……..nitric oxide

PDE ……phosphodiesterase

PGE_1…….. prostaglandin E_1

PIP_2…… phosphatidylinositol-4,5-bisphosphate

PKA…….. protein kinase A

PKC……protein kinase C

PLC…… phospholipase C

P_o……open probability

R……ratio

RA……. relative amplitude

RyR……... ryanodine receptor

SCD……sudden cardiac death

sGC…… soluble GC

siRNA…….small interfering ribonucleic acid

SR……...sarcoplasmic reticulum

wt……... wild type

CHAPTER 1: INTRODUCTION/LITERATURE REVIEW

Cellular Second Messengers

Distant cells can use chemical signaling to communicate with one another. Chemical signaling generally involves three components. A cell releases an extracellular signal, also known as a "first messenger." This first messenger binds to a specific receptor at the target cell, which can be located either in the membrane or cytoplasm, depending upon the chemical nature of the messenger. In response, the target cell may then mobilize yet another chemical signal, which is broadly referred to as a "second messenger." These second messengers may cause downstream effects to modulate biological functions or they may serve to mobilize additional second messengers (Reviewed in Beavo and Brunton, 2002).

Many second messengers are well conserved across cell types. For example, G-proteins can activate phospholipase C (PLC) to catalyze the breakdown of phosphatidylinositol-4,5-bisphosphate (PIP_2) into two second messengers: inositol-1,4,5-trisphosphate (IP_3) and diacylglycerol (DAG). DAG, in conjunction with calcium (Ca^{2+}), activates a class of phospholipid-dependent kinases known as protein kinase C (PKC). PKC phosphorylates many cellular proteins to exert its cellular effects. Additionally, the IP_3 liberated from PIP_2 works through a separate pathway to cause the release of Ca^{2+} from intracellular stores (Reviewed in Oude Weernink et al., 2007). Ca^{2+}, in turn, binds to troponin C in cardiac and skeletal muscle, and activates calmodulin in most cells. The binding of Ca^{2+}/calmodulin by Ca^{2+}/calmodulin dependent kinase (CaM kinase) activates the kinase, which phosphorylates a variety of cellular proteins (Reviewed in Maier and

Bers, 2007) as well as directly activates enzymes such as phosphodiesterases and adenylyl cyclase (Reviewed in Iacovelli et al., 1999).

cAMP

Another important, and ubiquitous, second messenger is cyclic adenosine monophosphate (cAMP). Earl Sutherland made some early advances in this field while researching how hormones like epinephrine promote glycogenolysis. Rall et al (1956) discovered that activation of liver phosphorylase was accompanied by the incorporation of phosphate into the enzyme. By 1958, the messenger cAMP, adenylyl cyclase (AC), which synthesizes cAMP, and phosphodiesterases (PDEs), which degrade cAMP, had all been described (Reviewed in Beavo and Brunton, 2002).

Krebs and colleagues found that epinephrine stimulated a cascade of kinases, the first of which was activated by cAMP (Reviewed in Krebs and Beavo, 1979). This completed the pathway from hormone to glycogenolysis. Subsequent investigations by many investigators demonstrated that many additional cellular substrates could also be phosphorylated by this cAMP-activated protein kinase, which was renamed protein kinase A (PKA) (Langan, 1968; Lohmann et al., 1980).

Other studies investigated PDEs, the enzymes responsible for hydrolyzing cAMP. Early studies suggested that the maximal rate of cAMP degradation was greater than synthesis by more than an order of magnitude. Regulation of PDE activity occurs via a variety of mechanisms, and is often quantitatively more important in controlling cAMP levels than the rate of synthesis (Reviewed in Beavo and Brunton, 2002).

PDEs

PDEs possess conserved C-terminal and catalytic domains and unique N-terminal domains which are important for subcellular localization (Lenhart et al., 2005). There are 11 families and more than 90 isoforms of PDEs (Zaccolo and Movsesian, 2007). There are at least five families of PDEs expressed in the neonatal rat ventricular myocytes: PDE1, PDE2, PDE3, PDE4 and PDE5 (Mongillo and Zaccolo, 2006).

PDE1 is activated by Ca^{2+}/calmodulin and can hydrolyze either cGMP or cAMP. PDE2 can be activated by cGMP and can also hydrolyze cGMP or cAMP (Rochais et al., 2006). PDE2 is reported to be responsible for blocking the increase in cAMP generated by β-adrenergic stimulation in cardiac myocytes (Mongillo et al., 2006). PDE3 and PDE4 provide the major cAMP hydrolytic activity in the heart (Mongillo et al. 2004). PDE3 is inhibited by cGMP and preferentially hydrolyzes cAMP whereas PDE4 is cAMP specific (Rochais et al., 2006). PDE3 is responsible for most of the cAMP hydrolyzing activity in membrane-enriched fractions of human myocardium. Its contribution to cytosolic cAMP hydrolysis varies from greater than 50% to less than 20%, depending on the experimental conditions (Zaccolo and Movsesian, 2007). In a fluorescence resonance energy transfer (FRET) study of neonatal rat cardiac myocytes, Mongillo et al. (2004) found that PDE3 and PDE4 contributed approximately 90% of cAMP hydrolyzing activity. Of this 90%, PDE4 contributed twice as much as PDE3. They found that approximately 90% of PDE4 activity was from the PDE4B and PDE4D isoforms, and that of this, PDE4D contributed twice as much as PDE4B (Mongillo et al., 2004).

PDE5 is cGMP specific and as such does not hydrolyze cAMP. It has been shown to be expressed in the heart (Nagendran et al., 2007), although it is unknown

whether it is involved in regulating cardiac contractility. However, PDE5 inhibition counteracts the cAMP-mediated effects of catecholamine (β-adrenergic) stimulation, and further investigation could lead to a better understanding of its purpose (Reviewed in Mongillo and Zaccolo, 2006).

Clinical use of PDE Inhibitors

A characteristic of heart failure is reduced cAMP levels, especially in the terminal stages of the disease (Packer et al., 1991). As such, it would seem logical to attempt to elevate cAMP levels as a treatment of heart failure. The elevation of cAMP can be achieved by one of two ways: either 1) by increasing cAMP production; or 2) by inhibiting cAMP degradation. However, treatments which elevated cAMP are known to actually exacerbate heart failure and further promote arrhythmias (Packer et al., 1991). The effect of milrinone, a PDE3 inhibitor, on the treatment of heart failure was investigated in a clinical study. It was found that there was a 34% increase in cardiovascular mortality with respect to controls in patients taking milrinone. Additionally, there was a 53% increase in mortality in patients whose heart failure symptoms were the most severe at the start of treatment (Packer et al., 1991). In fact, milrinone was so deleterious to patient survival that the study was stopped before its scheduled completion.

In addition to milrinone, similar observations are reported with other PDE inhibitors. For example, theophylline, which is used to treat asthma and chronic obstructive pulmonary disease (COPD), also causes an increase in mortality due to arrhythmias (Bittar and Friedman, 1991). In addition to PDE3 inhbitors, PDE4 inhibitors

are used to treat asthma, COPD and Alzheimer's disease (Lehnart et al., 2005). Consequently, because of the potential role of PDE deficiency in heart failure, and the known cardiac side-effects of PDE inhibitors used to treat other clinical conditions, it is important to understand PDE regulation in the heart.

G-protein coupled receptor signaling

G-protein coupled receptors (GPCRs) consist of a protein with seven trans-membrane domains bound to the Gα subunit of a heterotrimer, which consists of Gα, GDP and Gβγ. The binding of a ligand to the GPCR causes Gα-GDP to exchange GDP for GTP which in turn causes Gα-GTP and Gβγ to dissociate from the receptor and each other. Gα-GTP and Gβγ are subsequently able to activate downstream elements, such as adenylyl cyclase (AC), which produces cAMP (Reviewed in Hendrickson, 2005).

In the heart, the major pathway for increasing intracellular cAMP is catecholamines binding to β-adrenergic receptors (β-AR), which are GPCRs. The cAMP activates PKA, which in turn phosphorylates many targets such as the L-type calcium channels ($I_{Ca,L}$) of the sarcolemma. Phosphorylation of these channels results in an increased open probability (P_o) at the single channel level, causing a global increase in $I_{Ca,L}$ and contractility (Reviewed in Brette et al., 2005) via calcium-induced calcium release (CICR). Additionally, β-adrenergic signaling directly increases the P_o of ryanodine receptors by activating muscle A-kinase anchoring protein (mAKAP)-bound PKA, which phosphorylates these sarcoplasmic reticulum channels (Marx et al., 2000; Wehrens et al., 2003).

Ligands which use similar second messenger pathways can have very different effects at the cellular level. Rochais et al. (2006) noted that different GPCRs have different effects on contractility and glycogen metabolism in the heart despite using a common second messenger pathway. For example, both the β_1-AR and the E-prostanoid (EP) 1 receptor are GPCRs that act via a cAMP/PKA cascade, but β_1-adrenergic stimulation causes increased force of contraction and stimulation of glycogen phosphorylase while prostaglandin E_1 (PGE_1) has no effect on contractile activity or glycogen metabolism. Consequently, the different effects of ligands which use similar second messenger pathways has lead to the idea that these second messenger pathways must be segregated from one another.

β-adrenergic receptors

There are three β-adrenergic receptor (β-AR) subtypes expressed in the mammalian heart: β_1, β_2 and β_3 (Nikolaev et al., 2006). β_1-ARs comprise 75-80% of β-ARs in mammalian hearts (Rybin et al., 2000). β_1 and β_2 are primarily involved in mediating the increase in chronotropy and inotropy associated with β-adrenergic stimulation of the heart. These receptors couple primarily to G_s, which promotes cAMP production and PKA-dependent phosphorylation of various components of the excitation-contraction coupling (ECC) machinery. Targets for PKA derived from β-adrenergic stimulation include the L-type calcium channel, phospholamban, the RyR and troponin T and I. Evidence has been found supporting differential compartmentation of β_1- and β_2-mediated cAMP signaling, with localized control of cAMP degradation supplied by PDEs (Nikolaev et al., 2006).

Nikolaev et al. (2006) set out to elucidate differences between cAMP generated by β_1 and β_2 stimulation in adult mouse cardiac myocytes. They conducted their experiments in ventricular myocytes from transgenic mice expressing a novel cAMP-FRET sensor. This sensor was based on the hyperpolarization activated cyclic nucleotide-gated cation channel 2 (HCN2), and was distributed in the cytosol. Using the non-specific β-adrenergic agonist isoproterenol in the presence of phosphodiesterase inhibitors, they found that cAMP generated by β-adrenergic stimulation was primarily regulated by PDE4, with less significant contributions by PDE2 and less still by PDE3. Furthermore, cAMP generated by β_1-AR stimulation was primarily regulated by PDE4, while cAMP generated by β_2-AR was regulated by multiple PDEs.

They also found that there was twice as much cAMP generated by β_1-AR stimulation as by β_2-AR stimulation, even in the presence of complete PDE inhibition by 3-isobutyl-1-methylxanthine (IBMX). Additionally, cAMP generated by the β_1-AR propagated throughout the cell over a distance spanning multiple sarcomeres, while cAMP generated by the β_2-AR remained locally confined. Interestingly, the compartmentation of β_2-AR generated cAMP was also G_i independent. Disruption of G_i inhibitory G proteins with pertussis toxin did not alleviate the limited diffusion of β_2-AR generated cAMP. The experimenters concluded that there must be additional mechanisms restricting cAMP generated by the β_2-AR which are PDE and G_i independent, such as differential receptor localization with respect to caveolae and t-tubules (Nikolaev et al., 2006).

Co-localization to caveolae

Caveolae are 50 to 100nM deep plasma membrane invaginations enriched in cholesterol, sphingolipids and the protein caveolin. Caveolin-3 (Cav-3) is the primary isoform expressed in muscle (Balijepalli et al., 2006). Caveolae may play a role in membrane receptor internalization; it has been suggested that GPCRs can be phosphorylated by PKA and internalized from these regions. In addition to the plasma membrane, caveolae may also be localized to intracellular membranes such as the SR and t-tubules. Interestingly, GPCRs and post-receptor agonists appear to localize differently in the caveolin-rich fraction of adult cardiac myocytes versus fibroblasts, smooth muscle cells and neonatal cardiac myocytes (Insel et al., 2005). The latter suggests that there may be a developmental component to GPCR localization as well as the mechanisms of second messenger compartmentalization. In the heart, several signaling molecules have been localized to caveolae, including the β_2–AR, the voltage-dependent Na channel, the voltage-dependent potassium channel $K_v1.5$, the Na/Ca^{2+} exchanger and the HCN4 pacemaker (Balijepalli et al., 2006).

Rybin et al. (2000) set out to determine whether or not caveolae are a location for compartmentalized β-AR signaling in cardiac myocytes. Using immunoblot analysis of proteins extracted from neonatal rat cardiac myocytes, they found that β_1-ARs localize to caveolae, non-caveolar cell surface plasma membrane and internal membranes. Along with more than 99% of cellular proteins, the vast majority of β_1-ARs were non-caveolar. On the other hand, β_2-ARs localize to caveolae. Additionally, β_2-ARs localize to caveolae and internal membranes in cardiac fibroblasts, and were excluded from non-

caveolar plasma membrane, indicating that this may be a general phenomenon. They also found that isoproterenol-stimulated trafficking from caveolae was limited to β_2-ARs.

Rybin et al. (2000) subsequently went on to explore the localization of downstream elements in the β-AR signaling cascaded. The vast majority of $G\alpha_i$ subunits and approximately 50% of $G\alpha_s$ and β subunits were found in caveolae. Additionally, as much as 50% of AC localizes to caveolae, where it interacts with Cav-3. Caveolae contained negligible amounts of the α-catalytic and RI regulatory subunits of PKA, but were highly enriched in the RII regulatory subunit. Finally, disassembly of caveolae using cyclodextrin increased cAMP accumulation in response to β_1, β_2 and direct AC activation with forskolin. As such, it is possible that caveolae act to inhibit cAMP formation with inhibitory control at the level of AC. Evidence supporting this is provided by the fact that AC6 can be inhibited by capacitive calcium entry through channels that co-localize to caveolae (Rybin et al., 2000).

Recruitment of PDEs to β-ARs

GPCR uncoupling limits the magnitude of agonist-induced signals, and returns cells to an un-stimulated state. Uncoupling occurs through desensitization, whereby activated receptors are phosphorylated and subsequently bind to β-arrestin proteins (Perry et al., 2002). These proteins inhibit further receptor interaction with G-proteins. β-arrestins can also recruit cytosolic proteins to the plasma membrane, a phenomenon which Perry et al. (2002) chose to investigate further. They administered isoproterenol to HEK cells over-expressing G_s and AC-coupled β_2-AR. They found that there was a similar time-course for the recruitment of the major PDE4 isoforms expressed in these

cells to the plasma membrane as for the recruitment of β-arrestins. They also challenged cells over-expressing PDE4D3 and β_2-AR with isoproterenol, and found that there was a similar time-course for the recruitment of PDE4D3 and β-arrestins to β_2-AR. Additional studies demonstrated that there was no PDE4 recruitment to membranes upon isoproterenol stimulation of mouse embryonic fibroblasts which expressed β-ARs but lacked β-arrestin 1 and 2. In this study, wild-type levels of exogenous β-arrestin 1 re-established normal PDE4 recruitment to the membrane (Kohout et al., 2001).

Perry et al. (2002) subsequently used immunoprecipitation to demonstrate an association between β-arrestins and PDE4s. Experiments revealed the presence of complexes containing both PDE4D3 and β-arrestin 1 in Rat-1 cell cytosol. In accordance with a characteristic common to PDEs, PDE4D1 to 5 have identical catalytic and carboxyl termini but different amino termini which are responsible for interactions with scaffolding and signaling proteins. β-arrestin 1 and β-arrestin 2 expressed in COS-7 cells immunoprecipitated with all five isoforms of PDE4, suggesting that the common catalytic and carboxyl domains are involved in the association between PDEs and β-arrestins. Finally, the experimenters set out to determine the effects of overexpressing a mutant PDE4D5 with negligible catalytic activity that could still bind to β-arrestins in COS-7 cells. As such, this mutant PDE4D5 competed with wt PDE4D5 for binding to β-arrestins. Overexpression of mutant PDE4D5 increased isoproterenol-stimulated membrane PKA activity in relation to mock-transfected cells. In light of these results, it was concluded that β-arrestins recruit PDEs to ligand-activated receptors, thereby targeting cAMP degredation to plasma membrane sites of localized PKA activation

(Perry et al., 2002). As such, β-arrestins play a role in attenuating PKA activation in addition to their role in receptor desensitization.

cAMP-cGMP pathway cross-talk

In addition to cAMP, cGMP is an important regulator of cardiac function. Nitric oxide (NO) and atrial natriuretic peptides activate guanylyl cyclase (GC) to produce cGMP (Zaccolo and Movsesian, 2007). There are two forms of GC: soluble GC, which is found in the cytosol and activated by NO, and particulate GC, which is localized to the membrane and activated by natriuretic peptides. cGMP, in turn, activates downstream effectors such as PKG and cyclic nucleotide-gated channels to mediate changes in inotropy and metabolic responses. cAMP- and cGMP- mediated pathways often have opposing effects on cardiac function, in part due to the opposite consequences of PKA and PKG phosphorylation of target proteins. As was previously mentioned, cGMP can also serve as a regulator of cAMP hydrolyzing PDEs (Zaccolo and Movsesian, 2007).

A potential mechanism for cGMP regulation of cAMP pathways involves the differential sensitivities PDEs for cGMP. Low levels of cGMP (< 50nM) inhibit PDE3, while intermediate levels (200nM < cGMP < 500nM) would also activate PDE2. At higher levels of cGMP (> 1μM), PDE1 inhibition could also occur, although this has not been demonstrated *in vivo* (Zaccolo and Movsesian, 2007). The presence of cGMP anchoring proteins as well as restricted cGMP diffusion suggests the potential for cGMP compartmentation, similar to that proposed for cAMP (Zaccolo and Movsesian, 2007). The differential sensitivity of cAMP-hydrolyzing PDEs to cGMP and the potential for

cGMP compartmentation suggest a mechanism whereby distinct cGMP pools could regulate PDEs and their associated pools of cAMP in cardiac myocytes.

A specific example of cAMP and cGMP pathway crosstalk is provided by the work of Mongillo et al. (2006). They set out to investigate the effects of PDE2 activity on the β-AD-mediated increase in cAMP using neonatal rat ventricular myocytes expressing a genetically encoded cAMP sensor. As previously noted, PDE2 is a cGMP-activated cAMP-hydrolyzing PDE. Specifically, PDE2 increases its hydrolytic activity in response to cGMP binding to its N-terminal paired GAF domains. In a series of FRET experiments, Mongillo et al. (2006) found that inhibition of PDE2 with the specific inhibitor erythro-9-(2-hydroxy-3-nonyl)adenine (EHNA) and stimulation with NE resulted in a similar increase in cAMP compared to complete PDE inhibition with IBMX. However, the effects of EHNA were more than 30 times greater when the cAMP was produced by NE stimulation than direct AC activation with forskolin. Using immunocytochemsitry and confocal microscopy, they found that PDE2 localized to the plasma membrane, in particular to cell to cell junctions and the sarcomeric Z-line (Mongillo et al., 2006).

It has also been determined that NO activation with SNP decreases cAMP produced by NE, while soluble GC (sGC) inhibition with ODQ reverses this effect. PDE2 inhibition prevents SNP and ODQ from altering NE-generated cAMP levels, indicating that an NO-dependent pathway may act through PDE2 to increase hydrolysis of cAMP. Additionally, NE administration produced a similar amount of cGMP regardless of whether β_1 and β_2 were blocked, leaving only the β_3-AR active (Mongillo et al., 2006). Furthermore, β_3 inhibition increased cAMP generated in response to NE.

Mongillo et al. (2006) subsequently explored the functional consequences of PDE2 inhibition on adult mouse ventricular myocytes. They found that there was increased fractional cell shortening and calcium transients with PDE2 inhibition and NE as opposed to NE alone, and that these effects were significantly attenuated in endothelial nitric oxide synthase (eNOS) homozygous knockout mice. There was no effect on fractional cell shortening and calcium transients in the presence of PDE2 inhibition when the cAMP was produced by direct activation of AC by forskolin (Mongillo et al., 2006).

In light of these results, the experimenters proposed a pathway whereby NE activation of the β_3-AR stimulates eNOS to produce NO. NO, in turn, activates sGC to produce cGMP, which enhances PDE2 hydrolysis of cAMP produced by β_1 and β_2-ARs in response to catecholaminergic stimulation (Mongillo et al., 2006). Consequently, this study provides an example of cGMP-mediated attenuation of cAMP signaling, and of crosstalk between the two pathways.

Cardiac Excitation-Contraction Coupling and G-Proteins

Many of the key elements involved in ECC and hormonal regulation of contractility in heart cells are located at the t-tubules (Laflamme and Becker, 1999). T-tubules are invaginations in the surface membranes of mammalian cardiac myocytes that occur at the Z-line and are closely associated with the junctional sarcoplasmic reticulum (SR). L-type calcium channels and ryanodine receptors (RyRs), the SR calcium release channels involved in CICR and ECC, are found primarily at the t-tubules (Reviewed in Brette and Orchard, 2003). The key elements of the β-adrenergic signaling cascade such as Gs and AC are also concentrated at the t-tubules (Laflamme and Becker, 1999).

Like many of the components of ECC and β-adrenergic signaling, PDE4 enzyme-activity is also located in the vicinity of the t-tubules and junctional SR in mammalian cardiac myocytes. For example, PDE4D3 binds to mAKAPs in a complex which contains PKA (Dodge et al., 2001; Lehnart et al., 2005). mAKAP is also bound to the RyR, and PKA phosphorylation increases the P_o of the RyR. The presence of this macromolecular signaling complex provides a mechanism whereby cAMP access to PKA can be both spatially and temporally regulated by PDE4D3, and also whereby cAMP produced by β-adrenergic signaling can be localized and degraded (Dodge et al., 2001; Lehnart et al., 2005).

The RyR macromolecular signaling complex

Another important target for cAMP signaling with important consequences for contractility and disease states is the RyR macromolecular signaling complex. Brillantes et al. (1994) conducted an important study of the skeletal muscle RyR channel and its stabilization by the FK506-binding protein FKBP12. The RyR is composed of four subunits, each of which binds one FKBP12. In the absence of FKBP12, single channel recordings provide evidence for partial cooperativity between the four subunits in the form of subconductance states. The expression of FKBP12 in insect cells eliminated subconductance states, possibly because the prolyl isomerase activity of FKBP12 maintains proper folding of the RyR subunits. RyR co-expressed with FKBP12 had a decreased P_o but an increased mean open time, optimal parameters for calcium release into the cytoplasm. Interestingly, drugs which interfered with the prolyl isomerase action of FKBP12 induced muscle twitches in skeletal muscle preparations, indicating some

physiological effects of destabilization of the RyR channel in skeletal muscle (Brillantes et al., 1994).

A subsequent study examined the regulation of FKBP12.6 binding to the RyR2 and how this could be modified in disease states. They found that FKBP12.6, the PKA catalytic subunit, R2 (the PKA regulatory subunit), phosphatases PP1 and PP2A and mAKAP are in a molecular complex with the RyR2, (Marx et al., 2000). Based on these findings, they proposed that PKA phosphorylation of RyR2 causes FKBP12.6 to dissociate from the complex, increasing P_o of RyR2 by increasing its sensitivity to calcium-dependent activation. Consequently, this provides a possible mechanism whereby β-adrenergic cAMP signaling exerts its effects on contractility.

Marx et al. (2000) also investigated the characteristics of RyR2 in pathophysiological conditions. They found that RyR2 was hyperphosphorylated in heart failure, perhaps due to the observed decrease in phosphatases bound to the channel. Hyperphosphorylation resulted in the loss of FKBP12.6 from RyR2, subconductance states never seen in non-failing hearts and activation of RyR2 at resting levels of cytosolic calcium. These findings perhaps explain the blunted β-adrenergic response observed in heart failure: cAMP produced by β-adrenergic GPCRs is no longer able to cause PKA to phosphorylate RyR2 because the channel is already hyperphosphorylated.

Dodge et al. (2001) conducted an important study to determine the nature of the association between PKA, mAKAP and PDE4D3 in rat cardiac myocytes. They found that the PKA holoenzyme (composed of two regulatory subunits and two catalytic R2 subunits) and the phosphodiesterase PDE4D3 are bound to mAKAP and consequently proposed a mechanism for negative feedback of cAMP-dependent PKA activation. In

their model, PDE4D3 hydrolyzes low levels of cAMP to prevent basal activation of PKA. However, hormonal stimulation results in an increase in cAMP, which is able to activate PKA and cause the dissociation of the catalytic subunits from the regulatory subunits. The catalytic subunits then phosphorylate PDE4D3, thereby increasing its activity. The activated PDE4D3 hydrolyzes cAMP to cause the reformation of the PKA holoenzyme (Dodge et al., 2001).

The work of Dodge et al. (2001) has many interesting implications in the context of previous work by Marx et al. (2000). As was previously mentioned, Marx et al. (2000) found that mAKAP was part of the RyR macromolecular signaling complex and that hyperphosphorylation of the channel was a characteristic of heart failure. Consequently, Dodge et al. (2001) hypothesized that disruption of PDE could lead to hyperphosphorylation of RyR and the leaky channels characteristic in heart failure by removing the feedback inhibition on the activation of PKA.

The L-type Ca^{2+} channel

There is also evidence that cAMP-signaling at the L-type Ca^{2+} channel shares some features with cAMP-signaling at the RyR. Hulme et al. (2003) conducted a study to determine the role of A-kinase anchoring proteins (AKAPs) in targeting PKA to $Ca_V1.2$ channels, the major L-type Ca^{2+} channel in the heart. It was demonstrated that AKAP15 targets PKA to the C-terminus of $Ca_V1.1$ in skeletal muscle via a leucine zipper (LZ) interaction. In a sequence alignment of the C-terminus of $Ca_V1.1$, they found that the LZ domain is conserved throughout Ca_V1. Additionally, $Ca_V1.2$ coimmunoprecipitated with AKAP15 from rat heart extracts as well as transfected tsA-

201 cells (Hulme et al., 2003). AKAP15 also coimmunprecipitated with the C-terminal domain of $Ca_V1.2$ expressed on its own in tsA-201 cells. However, this interaction was lost with mutations in $Ca_V1.2$ or AKAP15 that disrupted the putative LZ domain. Using immunofluorescence, Hulme et al. (2003) determined that $Ca_V1.2$ and AKAP15 co-localize at the t-tubules in rat ventricular myocytes. Finally, they determined that inhibiting the PKA-AKAP15 interaction using HT31 or the AKAP- $Ca_V1.2$ interaction using $AKAP15_{LZ(38-54)}$ (the leucine zipper domain of AKAP15) attenuated the isoproterenol-mediated increase in $I_{Ca,L}$. This was not seen in with the addition of an $AKAP15_{LZ(38-54)}$ LZ mutant to the pipette solution. Consequently, they proposed that an LZ domain on the C-terminus of $Ca_V1.2$ anchors PKA via AKAP15 to mediate the β-adrenergic increase in $I_{Ca,L}$ in heart cells (Hulme et al. 2003). While it is currently unknown if a PDE is associated with the AKAP15-PKA complex, its presence would not be surprising given previous studies of cAMP signaling and RyR2.

Calcium Channels of the Sarcolemma

In cardiac myocytes, a significant fraction of L-type Ca^{2+} channels are localized to the t-tubules in close proximity to SR Ca^{2+} release channels. However, they are also found on the surface sarcolemma (Balijepalli et al., 2006). Using immunofluorescence labeling, it was found that $Ca_v1.2$ (the pore forming unit of the L-type Ca^{2+} channel) and Cav-3 co-localize on surface membrane domains and punctuate areas consistent with t-tubules in cardiac myocytes. They also found that both proteins colocalize to caveolae in cardiac myocytes using immunogold labeling and electron microscopy, which provides better spatial resolution than confocal microscopy. $Ca_v1.2$ immunoprecipitated with β_2-

AR, $G\alpha_s$, AC, $PKA_{RII,}$ and PP2A, but not β_1-AR or $G\alpha_i$, while Cav-3 immunoprecipitated with the same proteins as well as $G\alpha_i$ (Balijepalli et al., 2006). This suggests that caveolar $Ca_v1.2$ channels are part of a macromolecular signaling complex.

Electrophysiological experiments were subsequently performed on neonatal mouse ventricular myocytes. Balijepalli et al. (2006) disrupted G_i with pertussis toxin in order to determine the effects of β_2-AR stimulation on $I_{Ca,L}$. β_2-AR stimulation of $I_{Ca,L}$ was eliminated by disruption of caveolae with methyl-beta cyclodextrin (MBCD) whereas β_1-AR stimulation of $I_{Ca,L}$ was unaffected. These results were confirmed by small interfering ribonucleic acid (siRNA) directed against Cav-3, which eliminated the effect of β_2-AR stimulation on $I_{Ca,L}$. The results of this study indicate that there are a subpopulation of L-type Ca^{2+} channels localized to caveolae as part of a macromolecular signaling complex necessary for β_2-AR regulation of $I_{Ca,L}$ (Balijepalli et al., 2006).

Along with the work of Nikolaev et al. (2006) and Rybin et al. (2000), the work of Balijepalli et al. (2006) indicates that factors other than the localization of PDEs can be important in the compartmentation of second messenger pathways. Specifically, these results suggest that there may be different ways of regulating Ca^{2+} channel/β-AR interactions in the caveolae (mostly β_2-AR) versus the ECC associated t-tubules (β_1-AR), the latter which seems to rely more heavily on PDEs to localize the cAMP signal.

Role of PDEs and associated proteins in disease states

In light of the potential clinical applications of the aforementioned research, the effect of FKBP12.6 deficiency on arrhythmias has been studied (Wehrens et al., 2003). Ventricular arrhythmias can be rapidly fatal, a phenomena known as sudden cardiac

death (SCD). SCD is responsible for approximately 50% of deaths in heart failure, and is associated with many common cardiac diseases. Triggered arrhythmias can be caused by delayed after depolarizations (DADs), which are premature depolarizations after repolarization of the cardiac action potential due to aberrant SR calcium release.

During exercise, catecholamines activate β-ARs in the heart. Catecholaminergic polymorphic ventricular tachycardia (CPVT) is an arrhythmogenic disorder of the heart characterized by ventricular tachycardia during exercise but not at rest. Mutations in the gene coding for human RyR2 are associated with this disease (Wehrens et al., 2003).

It has been shown that FKBP12.6$^{-/-}$ mice displayed exercise-induced ventricular arrhythmias similar to those in CPVT (Wehrens et al., 2003). Heart cells from these mice showed DADs upon the administration of catecholamines. Additionally, RyR2 channels from FKBP12.6$^{-/-}$ mice which had exercised showed subconductance states and had a greater P_o than controls. Wehrens et al. (2003) also expressed three mutant RyR2 channels associated with CPVT in HEK 293 cells. These cells showed depletion of FKBP12.6 from the RyR2 complex and increased P_o with PKA phosphorylation, which mimics the effect of exercise-induced β-AR signaling in humans. They proved that the lack of FKBP12.6 from RyR2 caused the observed subconductance states and increases in P_o by generating a mutant FKBP12.6 which could bind to phosphorylated RyR2 channels. This mutant bound to RyR2 in exercised FKBP12.6$^{-/-}$ mice as well as CPVT RyR mutant channels treated with PKA and abolished the previously observed subconductance states and elevated P_o.

It is interesting to note that the depletion of FKBP12.6 from the RyR2 macromolecular complex in the PKA-phosphorylated CPVT mutants in this study and the

RyR2 from failing human heart in their previous study (Marx et al. 2000) resulted in similar single channel properties, namely, subconductance states and increased P_o at low cytosolic calcium levels. In both cases, this may promote diastolic calcium leak and contribute to arrhythmias. Consequently, it is possible that the depletion of FKBP12.6 from RyR2, due to a mutation in CPVT or β-adrenergic hyperphosphorylation in heart failure, is a mechanism for triggered arrhythmias caused by diastolic calcium leak.

The role of PDEs in regulating cAMP signaling and the consequences of problems with this regulation has been further explored. It was determined that PDE4D3 is the only isoform of PDE4 found in the RyR2 complex and that PDE4D3 is decreased in humans with heart failure (Lehnart et al., 2005). They then created a $PDE4D3^{-/-}$ knockout mouse which was prone to age-related cardiomyopathy. The $PDE4D3^{-/-}$ knockout had increased PKA phosphorylation of RyR2 and decreased FKBP12.6 binding. Single channel recordings showed increased P_o with respect to wild type as well as subconductance states. The knockout mice were prone to exercise induced cardiac arrhythmias, whereas wt mice were not. In addition, wt mice treated with the PDE4-blocker rolipram and put on the exercise regimen had arrhythmias, which were not present in rolipram-treated RyR2-$S2808A^{+/+}$ knockin mutants that have a RyR2 channel which cannot be phosphorylated (Lehnart et al, 2005).

Further investigating the effect of $PDE4D3^{+/-}$ post-myocardial infarction (MI), it was found that these mice have a similar level of PDE4D3 in RyR2 as human heart failure patients. Crossing the $PDE4D3^{+/-}$ mice with RyR2-$S2808A^{+/+}$ or treating them with JTV-519, which enhances Calstabin 2 (FKBP12.6) binding, significantly improved cardiac performance post MI. RyR2 phosphorylation was significantly decreased post

MI in the PDE4D3$^{+/-}$ / RyR2-S2808A$^{+/+}$ cross and with JTV-519 treatment, and PDE activity in the RyR2 complex was increased with respect to PDE4D3$^{+/-}$ (Lehnart et al, 2005).

Taken together with their previous study of CPVT (Wehrens et al., 2003), this work by Lehnart et al. (2005) can help us form a general understanding about a way in which arrhythmias may be triggered in heart failure. In CPVT, exercise increases β-AR generation of cAMP, which triggers PKA to phosphorylate RyR2, causing the depletion of FKBP12.6 from the complex due to a mutation in the RyR2. This increases P_o of RyR2 and induces subconductance states and arrhythmias. β-AR stimulation is increased in heart failure, and it was shown that human heart failure patients exhibit a decrease in PDE4D3 in the macromolecular signaling complex (Lehnart et al., 2005). The increased β-AR stimulation results in the generation of cAMP, which triggers PKA to phosphorylate RyR2. The lack of PDE4D3 in heart failure prevents the attenuation of the β-AR signal, leading to the hyperphosphorylation of RyR2 and the depletion of FKBP12.6 from the complex. This increases P_o of RyR2 and induces subconductance states and, therefore, arrhythmias.

It would seem as if a potential cause of arrhythmias in CPVT and this model of heart failure is the depletion of FKBP12.6 from the RyR2 complex. In CPVT, this is due to a mutation in RyR2 which decreases FKBP12.6 binding with β-adrenergic stimulation. In the model of heart failure used by Lehnart et al. (2005), FKBP12.6 depletion is due to decreased PDE4D3 in the RyR2 complex. Heart failure is characterized by a hyperadrenergic state, and decreased PDE4D3 would result in the faulty termination of

the β-adrenergic cAMP cascade, hyperphosphorylation of RyR2 and depletion of FKBP12.6.

cAMP compartmentation

It is evident from the aforementioned discussion that regulation of cellular cAMP levels is complex and dynamic. This process is relevant to the normal functioning of every cell in the body and involved in disease states in specific organs such as the heart. However, there has been a question since the discovery that cAMP is involved in many cellular pathways; how can a conserved second messenger generate distinct responses to a wide variety of first messengers? It would appear there are several mechanisms controlling β-AD-mediated cAMP signaling, including differential receptor localization. However, there is mounting evidence that PDEs form an important locus for the regulation of cellular cAMP. In particular, there are studies supporting the idea that the distinct subcellular localization of PDEs is responsible for the creation of distinct cAMP signals in response to first messengers.

One of the first studies addressing the compartmentation of cAMP was conducted by Jurevicius and Fischmeister (1996). They found that the local application of isoproterenol, a β-AR agonist, resulted in a local increase in $I_{Ca,L}$, implying a local increase of cAMP. However, direct activation of AC by forskolin (FSK) resulted in widespread activation of $I_{Ca,L}$, implying the activation of a cAMP pathway which was not spatially limited. This also occurred when isoproterenol was applied in the presence of IBMX, a non-selective PDE inhibitor. It was concluded that PDE hydrolysis of cAMP around $I_{Ca,L}$ prevents diffusion, thereby compartmentalizing cAMP (Jurevicius and

Fischmeister, 1996). Consequently, their finding that cAMP could be compartmentalized by PDEs suggested a mechanism whereby pathways using cAMP could be segregated from one another and have different cellular effects.

Direct evidence for the compartmentation of cAMP signaling in cardiac tissue was provided by a fluorescence resonance energy transfer (FRET) study of neonatal rat cardiac myocytes (Zaccolo and Pozzan, 2002). It was reported that activation of the β-AR resulted in a local increase of cAMP in the vicinity of the t-tubules and junctional SR. PKA, a substrate for cAMP, was also anchored in this region via AKAPs. PDEs prevented cAMP diffusion, and PDE inhibition resulted in generalized activation of PKA. Importantly, only AKAP-anchored PKA could sense the change in cAMP produced by β-AR activation, suggesting a localized β-AR second messenger pathway (Zaccolo and Pozzan, 2002).

In a follow up FRET study, Mongillo et al. (2004) set out to determine which PDEs were involved in mediating the β-adrenergic cAMP signal. It was found that β-adrenergic stimulation by norepinephrine, in the presence of the PDE3 inhibitor cilostamide, resulted in a transient increase in cAMP. The transient nature of the increase in cAMP was possibly due to the activation of PDE4 by PKA. However, when they administered norepinephrine in the presence of the PDE4 inhibitor Ro 20-1724, they found that there was a stable increase in cAMP, implying that PDE4 was the PDE involved in mediating the β-adrenergic signal. They also determined that PDE3 was possibly localized on internal membranes while PDE4 was localized to the M-line and Z-line, where PKA was also found. It was concluded that PDE4, especially PDE4B2,

played a major role in the localization of the β-adrenergic cAMP signal, and that its specific subcellular localization could contribute to this role (Mongillo et al. 2004).

Rochais et al. (2006) compared the different cAMP signals generated by four different GPCRs; β_1-AR, β_2-AR, Glu-R and the EP1 receptor. By using high-affinity cyclic nucleotide-gated (CNG) channel mutants, they were able to directly monitor the concentration of cAMP below the plasma membrane in cultured adult rat ventricular myocytes. They found that blocking PDE3 or PDE4 increased the β_1-adrenergic cAMP signal, while blocking both PDE3 and PDE4 increased the β_2-adrenergic and PGE_1 cAMP signals. Blocking PDE4 increased the cAMP generated below the plasma membrane by glucagon.

The effect of PDE inhibitors downstream on $I_{Ca,L}$ was generally similar to that observed with the CNG channels. PDE3 and more prominently PDE4 control the effect of β_1-adrenergic and β_2-adrenergic stimulation on $I_{Ca,L}$ while PDE4 is responsible for limiting the effect of glucagon. PGE_1 did not have an effect on $I_{Ca,L}$ even with inhibition of PDE3 and PDE4, suggesting that cAMP generated by PGE_1 is not coupled to $I_{Ca,L}$. Because PDE inhibition generally had similar effects on cAMP generation and $I_{Ca,L}$, this study offers evidence that the regulation of cAMP by PDEs has important downstream consequences in cardiac myocytes (Rochais et al., 2006).

Conceptual models for PDE regulation of cAMP diffusion

There are two conceptual models for how PDEs regulate internal cAMP: PDEs act as a barrier to prevent cAMP diffusion from the site of synthesis or as a drain to prevent inappropriate activation of PKA by cAMP. Because cAMP is produced by

membrane-bound AC, the barrier model would involve a high concentration of cAMP at the plasma membrane which becomes progressively less concentrated further away from the membrane. The problem with this model is that plasma-bound PKA would be much easier to activate than PKA deep in the cytosol, as cAMP would have to pass through a PDE barrier at the membrane to activate cytosolic PKA. With regards to finely-tuned activation of particular PKA subsets, the question arises of how it would be possible to activate PKA deep inside the cell without concurrently activated PKA closer to the membrane (Reviewed in Zaccolo et al., 2006).

In the drain model, there is freely diffusing cAMP which can reach a significant concentration to activate PKA throughout the cell except where it is hydrolyzed by localized PDEs. As such, rather than acting as a barrier to prevent cAMP diffusion throughout the cell, PDEs would act, in the words of Zaccolo et al. (2006); "in defined compartments to protect sensitive targets from inappropriate activation." This model is plausible, although questions arise regarding the degree to which it allows for finely tuned regulation of PKA activation. As it is, the "drain" model could provide a useful conceptual framework for the analysis of functional data showing the effects of PDE disruption.

Hypothesis and Objectives

Based on the preceding discussion, it is evident that PDEs play an essential role in cardiac physiology and pathophysiology. It is also evident that β-AR signaling is quite complex and is in need of further investigation at the single cell level. Therefore, our goal is to examine the role of PDEs as a mediator for the actions of isoproterenol, a β-AR agonist, on unloaded cell shortening, calcium currents, calcium transients and SR calcium load. We will specifically examine the effects of PDE3 and PDE4 inhibition, as these families are well known to contribute to the vast majority of cAMP hydrolyzing activity in the heart, as well as the fact that highly specific blocking agents exist (Mongillo et al., 2004).

Our hypothesis is that the subcellular localization of different PDEs regulates distinct effects of isopoterenol on cellular contractility, calcium currents and calcium uptake and release from the SR. This compartmentation theory is based on previous studies that have suggested that PDE3 is associated with the membrane while PDE4 is localized to the Z-line (Mongillo et al., 2004, Lehnart et al., 2005).

There are several unique aspects of our study in relation to previously published work. Firstly, we are using freshly dissociated adult ventricular myocytes, whereas previous studies have used cultured ventricular myocytes (Rochais et al., 2006). Cardiac myocytes are notorious for phenotypic changes during culture, which is why these studies must be conducted with freshly dissociated cells (Reviewed in Mitcheson et al., 1998). Secondly, we are performing all electrophysiological experiments using the perforated patch clamp configuration, whereas previous studies have used whole cell (Rochais et al., 2006; Kerfant et al., 2007).

Calcium current rundown in whole cell (Belles et al., 1988; Korn and Horn, 1989; Fukumoto et al., 2005) due to dephosphorylation of L-type calcium channels (Ono et al., 1992) is well characterized in cardiac myoctyes. Additionally, whole cell is known for disrupting the internal cellular environment (Liem et al., 1995), which could be problematic when studying second messengers. We propose to avoid these difficulties using the perforated patch clamp technique.

CHAPTER 2: METHODS

Cell isolation

Cardiac myocytes were isolated from the right ventricular free wall of male Sprague-Dawley rats (225-275g) using the method of Ward and Giles (1997) with slight modifications. Animals were killed by decapitation using a protocol approved by the Queen's University Animal Care Committee in accordance with Canadian Council on Animal Care guidelines. The heart was rapidly removed and mounted on a cannula for retrograde perfusion at a rate of 10mL/min using standard Langendorff apparatus. The nominally Ca^{2+} -free Tyrode's solution contained (mM): NaCl 140; KCl 5.4; $MgCl_2$ 1; Na_2HPO_4 1; HEPES 5; glucose 10. The pH was adjusted to 7.4 with NaOH and continuously gassed with 100% O_2.

Hearts were initially perfused with standard Tyrode's solution containing 1 mM $CaCl_2$, followed by 5 min of perfusion with the Ca^{2+} -free Tyrode's solution. After this, the heart was perfused for 7-8 min with standard Tyrode's solution to which collagenase (0.02 mg/mL; Yakult Co. Ltd, Tokyo) and protease (0.004 mg/mL; Type XIV; Sigma) had been added. The right ventricular free wall was then removed and minced in 10mL of Tyrode's solution containing collagenase (0.5 mg/mL), protease (0.1 mg/mL), bovine serum albumin (BSA; 2.5 mg/mL; Sigma) and $CaCl_2$ (50 μM). The tissue was gently agitated in a shaker bath for 10-30 minutes at 37 ^{o}C until dissociated cells were observed. Once myocytes were present, aliquots were removed at 3 min intervals and stored in 4mL of modified KB solution containing (in mM): potassium glutamate 100; potassium aspartate 10; KCl 25; glucose 20; KH_2PO_4 10; HEPES 5; $MgSO_4$ 2; taurine 20; creatine 5; and EGTA 0.5; with 1mg/mL BSA, pH was adjusted to 7.2 with KOH.

Cell-Shortening recordings

To record unloaded cell shortening, which is representative of cardiac contractility, myocytes were field stimulated with a Grass SD9 stimulator at a rate of 1Hz. The video signal from the microscope was fed to an edge detection device (Crescent Electronics, USA). Output from the edge detection device was acquired using a pClamp 9.0 / Digidata 1320 data acquisition system and calibrated for cell length. Data are expressed as fractional unloaded cell shortening, which is defined as percent contraction of resting cell length with respect to t=0, the time immediately prior to isoproterenol (Sigma) administration.

Electrophysiological methods

Borosilicate glass electrodes were pulled on model P97, Sutter Instruments pipette puller. When filled with internal solution, pipette resistances ranged from 1 to 3 MΩ.

Cells were superfused with standard Tyrode's solution for potassium current recordings. The solution used to fill the pipettes contained (mM): KCl 20; K-Aspartate (L-Aspartic Acid) 110, EGTA 10, HEPES 10, $MgCl_2$ 1, K_2ATP 5, $CaCl_2$ 1, NaCl 10; pH was adjusted to 7.2 with KOH. These solutions created a junction potential of approximately 10 mV, which was compensated for.

Potassium currents were recorded during voltage clamp protocols using the perforated patch configuration. The transient outward (I_{to}), inward rectifier (I_{K1}), and delayed rectifier (I_{sus}) potassium currents were triggered using 500ms test pulses ranging from -120mV to +50mV, in 10mV increments, from a holding potential of -80mV. The

protocol was repeated with a pre-pulse to inactivate I_{to}, which consisted of a step to -40mV for 100ms immediately prior to the 500ms test pulses. The isolated I_{to} peak current amplitude was determined by subtraction of currents derived from the two protocols. I_{K1} currents were recorded with and without $BaCl_2$ (200μM), a selective inhibitor, from a holding potential of -80mV, with 500ms test pulses ranging from -120mV to +50mV, in 10mV increments. The I_{K1} current was derived by subtracting the resultant currents in the presence and absence of $BaCl_2$. I_{sus} measurements were taken from the residual current of the 500ms pulses recorded from -120mV to +50mV, in 10mV increments, from a holding potential of -80mV. I_{sus} was observed in isolation after 200μM $BaCl_2$ was applied, along with a 100ms pre-pulse to -40mV to eliminate I_{K1} and I_{to}, respectively. Action potentials were triggered using a 5ms, 700pA current injection.

For perforated patch calcium current recordings, the modified Tyrode's solution used for superfusion contained (mM): NaCl 140; CsCl 3; $CaCl_2$ 1; KCl 5.4, Na_2HPO_4 1; HEPES 5; glucose 10; $MgCl_2$ 1; Lidocaine 0.25 with pH adjusted to 7.4 with NaOH. The solution used to fill the pipettes contained (mM): CsOH 120; aspartic acid 120; CsCl 30; $MgCl_2$ 1; Na_2ATP 5; HEPES 10; EGTA 1; pH was adjusted to 7.2 with CsOH.

L-type Ca^{2+} currents were elicited at a rate of 0.1 Hz from a holding potential of -80 mV with a 1s ramp to -40 mV (to voltage inactivate sodium currents) followed by a 300 ms step to 0 mV to activate $I_{Ca,L}$. Currents were sampled at 10 kHz and filtered at 1 kHz. All data was acquired and analyzed with the pClamp 9.0/Digidata 1320 data acquisition system. All currents were initially expressed relative to cell capacitance and reported as current density (pA/pF). Data were subsequently expressed as fractional

current, which is defined as percent current with respect to t=0, the time immediately prior to isoproterenol administration.

For amphotericin-perforated patch recordings, a stock solution was made by sonicating 3 mg amphotericin B (Sigma) in 30 μL dimethylsulphoxide. Immediately prior to each experiment, 3.33 μL amphotericin stock was added to 1 mL of internal solution and sonicated briefly. When protected from light, this solution remained stable (for electrophysiological recordings) for up to 2 h. Prior to back-filling of the electrodes, the tips were dipped in amphotericin-free internal solution to enhance seal formation.

Calcium transient recordings

Rat myocytes were loaded with fluo-3 AM (Invitrogen/Molecular Probes, Carlsbad, CA) at 2.28 μM for 30 min in Ca^{2+}-free Tyrode's solution. Cells were superfused with a standard Tyrode's solution (Ca^{2+}-containing) for the recordings. Cells were visualized under oil immersion with a 100X objective (Nikon) and Type A oil (Fisher Scientific). For these experiments, we used an excitation wavelength of 480 nm using a Model 1600 Power Supply (Opti Quip), a model 720 lamp house with a 150W Xenon bulb and a DX-100 optical switch (Solamere Tech Group). Emitted fluorescence was recorded at 510 nm using a microfluorimeter and digitized using the pClamp 9.0 / Digidata 1320 data acquisition system. Calcium transients were elicited by field stimulating using a Grass SD9 stimulator at a rate of 1Hz. Changes in Fluo-3 AM fluorescence were expressed as a ratio (R) of fluorescence intensity (F) to the basal fluorescence intensity (F_0). Data are expressed as fractional fluorescence, which is

defined as percent fluorescence with respect to t=0, the time immediate prior to isoproterenol administration.

Caffeine-pulse experiments

Rat myocytes were loaded with fluo-4 AM (Invitrogen/Molecular Probes, Carlsbad, CA) at 2.3 µM for 15 min in Ca^{2+}-free standard Tyrode's solution. Cells were superfused with a Tyrode's solution (Ca^{2+}-containing) for the recordings. Fluo-4 was used in preference to fluo-3 due to prior experience with Fluo-3 for the calcium transient experiments. Fluo-4 permeates the cell membrane faster than Fluo-3 and is also a brighter dye, yielding higher resolution recordings (Gee et al., 2000). The cells were stimulated with a Grass SD9 stimulator at a rate of 1Hz for five minutes before the first caffeine-pulse recording. These five minutes were meant to serve as an equilibration period for the cells to attain a stable level of SR calcium.

To perform a caffeine pulse experiment, the stimulator and perfusion system were turned off while fluo-4 fluorescence was measured using the same wavelengths as those used for fluo-3. The cells were subsequently exposed to a rapid, unrestricted (gravity-limited) flow of Tyrode's solution containing 10mM caffeine, which causes release of the bulk of SR calcium (Su et al., 2003). At the end of the 75 or 90 second recording (recording time was selected to ensure the fluorescence level would return to a stable baseline), the caffeine perfusion was turned off, the stimulator was turned on and cells were again superfused with the standard Tyrode's solution. A second caffeine pulse experiment was performed 10 minutes after the standard Tyrode's superfusion was turned back on. Emitted fluorescence was recorded using a pClamp 9.0 / Digidata 1320 data

acquisition system. Area under the curve was taken as a measure of SR calcium content. Data are expressed as fractional fluorescence, which is defined as percent fluorescence with respect to t=0, the time immediate prior to isoproterenol administration.

Statistical Analysis

All statistical analysis was done using GraphPad Prism 4.0 software. Statistical analysis was performed using an ANOVA, followed by a Newman-Keuls post-hoc test when appropriate. An unpaired student's t test with two tails was used when there were only two values available for comparison. Data are considered statistically different with $P < 0.05$.

CHAPTER 3: RESULTS

In order to determine a concentration of isoproterenol that would allow us to observe the consequences of PDE inhibition on our experimental parameters, we constructed a concentration-response curve for the effects of isoproterenol on unloaded cell shortening (Figure 1). Rat cardiac myocytes were continuously field stimulated at a rate of 1 Hz. Various concentrations of isoproterenol, or vehicle control, were added to the superfusion solution and the effects recorded every two minutes over a ten minute period. No changes in unloaded cell shortening were observed in the control group (n=12). The addition of 1 nM isoproterenol lead to a small, insignificant increase in unloaded cell shortening to 114 ± 11 % (n=7) of t=0. In contrast, both of 3 nM (n = 8) and 10 nM isoproterenol (n = 7) caused significant increases in contractility, with increases to 190 ± 17 % and 265 ± 22 % of t=0, respectively. As can be seen with 30 nM isoproterenol (n=8), further increasing the concentration of isoproterenol did not lead to additional increases in unloaded cell shortening suggesting that the maximum contractility of these cells had been achieved. Additionally, at these higher concentrations, signs of calcium overload, such as spontaneous activity, became evident (Table 1).

Based on the concentration-response curve, we decided to use an isoproterenol concentration of 1nM in all subsequent experiments. This was selected since we predicted that inhibition of phosphodiesterase activity would potentiate the effects of β-adrenergic stimulation and we wished to use a level of stimulation that elicited sub-maximal effects on its own.

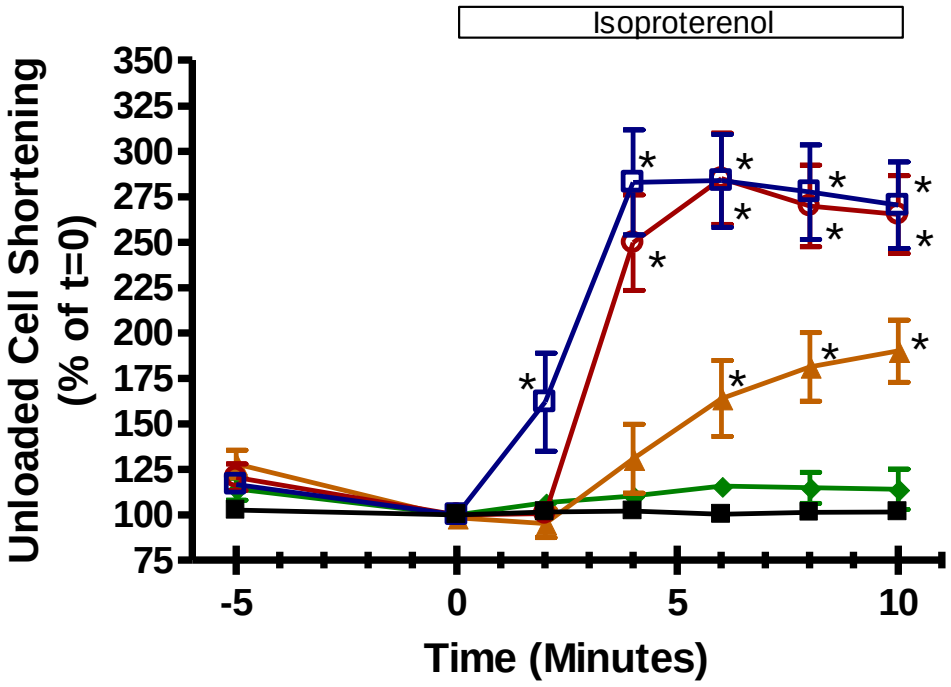

Figure 1. Concentration-dependent effects of isoproterenol on unloaded cell shortening. Cardiac myocytes were superfused with Tyrode's solution for five minutes prior to the addition of select concentrations [(0nM (black squares); 1nM (green diamonds); 3nM (orange triangles); 10nM (open red circles); 30nM (open blue squares)] of isoproterenol. Myocytes were continuously field stimulated at a rate of 1 Hz. Data are expressed as a percentage of unloaded cell shortening relative to time = 0, the time at which isoproterenol was added to the superfusion solution. Values represent the mean ± standard error of the mean for n = 7-12 experiments. (*) indicates data significantly different ($p<0.05$) from control values.

Table 1. Isoproterenol Unloaded Cell Shortening Dose Response Curve

	Overload at 20 Minutes			Overload before 20 Minutes		
Treatment	None	Partial	Complete	Complete	Died	Excluded
Control	12					
1nM Iso	7					2
3nM Iso	8				1	5
10nM Iso	3	8		1		9
30nM Iso	4	4	1	2		

To evaluate the effect of PDE inhibition on isopreterenol-stimulated increases in unloaded cell shortening, we selected two putatively selective PDE inhibitors. Cilostamide was chosen as a selective inhibitor of PDE3 while Ro 20-1724 was chosen as a selective inhibitor of PDE4 (Rochais et al., 2006). For these experiments, we recorded baseline shortening five minutes prior to the addition of either cilostamide (1 μM; Sigma), Ro 20-1724 (10 μM; Calbiochem) or vehicle control, followed by a five minute pre-treatment period prior to the cardiac myocytes being challenged with 1nM isoproterenol. Unloaded cell shortening was recorded immediately prior to the addition of isoproterenol and subsequently every two minutes over a 10 minute period. Representative data of these experiments is presented in Figure 2.

Pooled data demonstrating the effects of cilostamide pre-treatment on isoproterenol-stimulated increases of unloaded cell shortening are shown in Figure 3. As can be seen, addition of isoproterenol, following cilostamide pre-treatment, resulted in an increase of unloaded cell shortening to 216 ± 17 % (n=8) of t=0 at 10 minutes. This increase is significantly greater than that observed with isoproterenol alone, which was to 114 ± 11 % (n=7) of t=0 at 10 minutes. Repeating these experiments with Ro 20-1724 instead of cilostamide produced the results shown in Figure 4. In the presence of Ro 20-1724, 10 minutes exposure to isoproterenol increased unloaded cell shortening to 155 ± 12 % (n=8) of t=0. Figure 5 is a re-plot of the cilostamide + isoproterenol and Ro 20-1724 + isoproterenol data from Figures 3 and 4. As can be seen when the data are presented together, the effects of cilostamide were significantly greater than those of Ro 20-1724 between two and 10 minutes isoproterenol exposure. Overload was a minor factor in these experiments (Table 2).

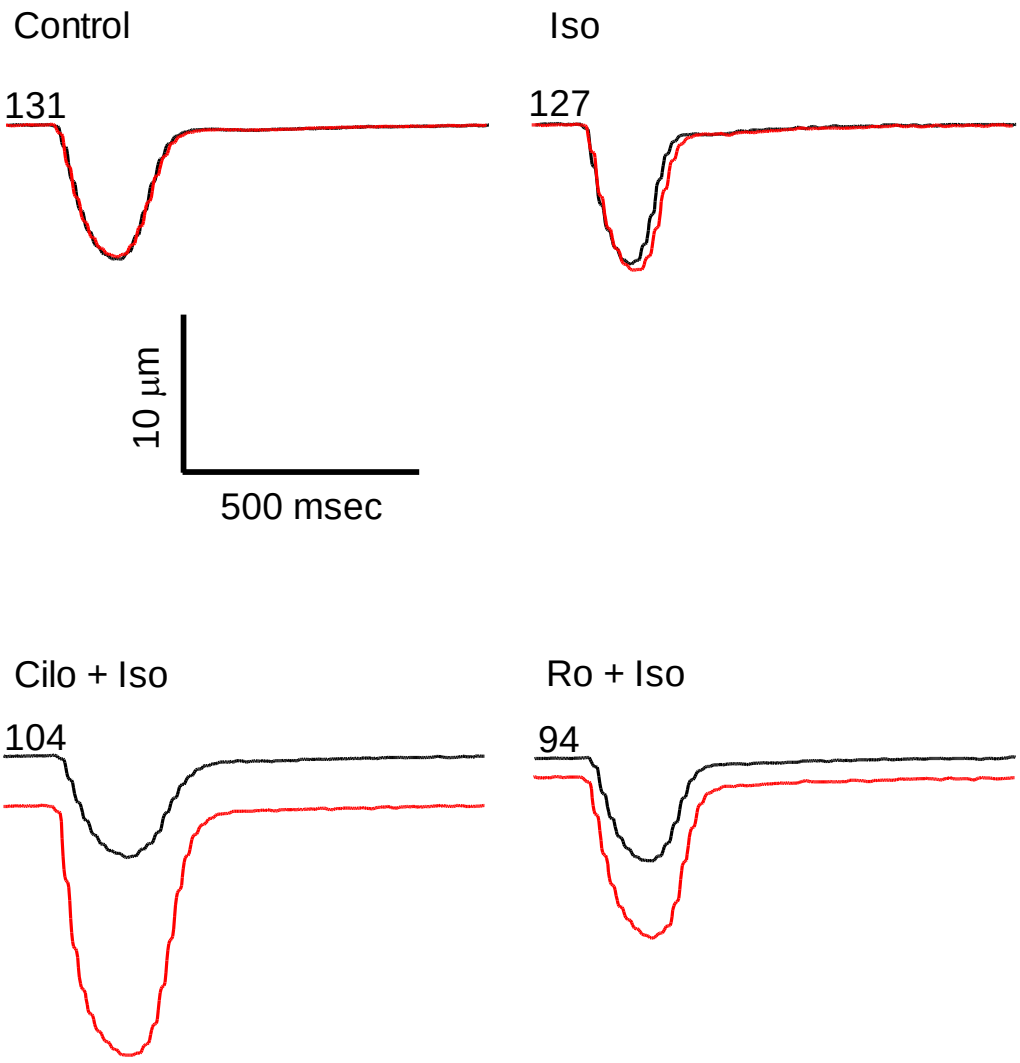

Figure 2. Representative data illustrating the effects of PDE inhibition on unloaded cell shortening. Cardiac myocytes were continuously field stimulated at a rate of 1Hz throughout the entire experiment. The effects of vehicle control (top left), isoproterenol alone (1 nM; top right), cilostamide and isoproterenol (1µM and 1 nM, respectively; bottom left) and Ro 20-1724 + isoproterenol (10µM and 1 nM, respectively; bottom right) are shown. Baseline shortening was recorded for five minutes prior to the addition of PDE inhibitors, followed by a five minute pre-treatment period prior to the cardiac myocytes being challenged with isoproterenol at t=0 minutes. Unloaded cell shortening was recorded immediately prior to the addition of isoproterenol and subsequently every two minutes over a 10 minute period. Sample traces were recorded at t=0 minutes (black) and t=10 minutes (red). Diastolic cell lengths (µm) at t=0 are listed above the baseline region in the sample traces.

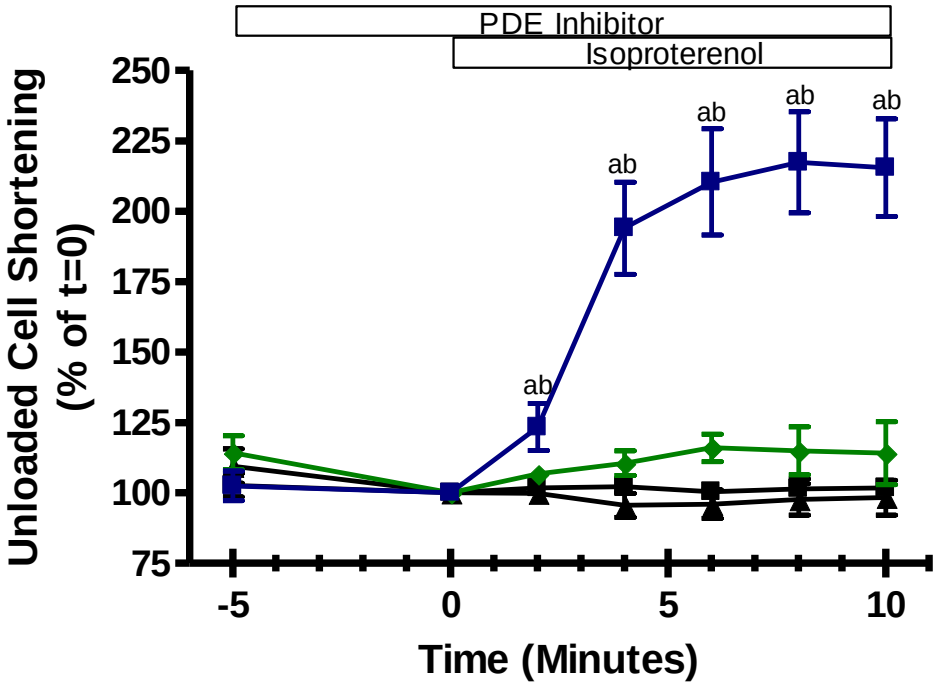

Figure 3. The effects of selective PDE3 inhibition on unloaded cell shortening. Cardiac myocytes were continuously field stimulated at a rate of 1Hz throughout the entire experiment. The effects of vehicle control (black squares), isoproterenol alone (1 nM; green diamonds), cilostamide alone (1 µM; black triangles) or both cilostamide and isoproterenol (blue squares) are shown. Bars on the graph indicate the times at which either cilostamide or isoproterenol were present. Data represent the mean ± standard error of the mean for n = 7-12 experiments and are expressed relative to unloaded cell shortening at t=0 minutes. (a) indicates data significantly different ($p<0.05$) from its appropriate control. (b) indicates data significantly different ($p<0.05$) than the isoproterenol only group.

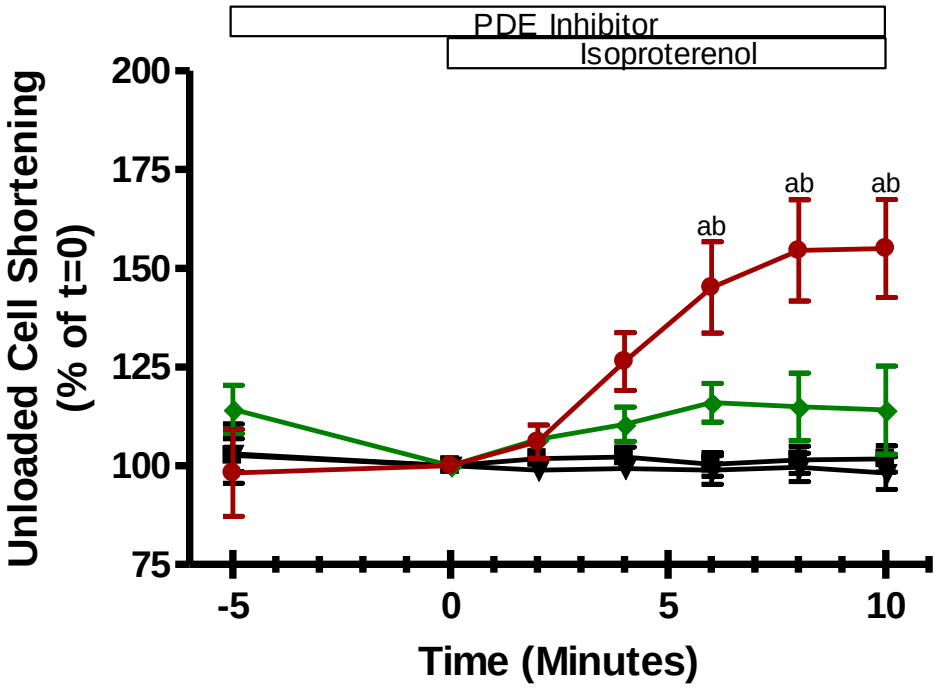

Figure 4. The effects of selective PDE4 inhibition on unloaded cell shortening. Cardiac myocytes were continuously field stimulated at a rate of 1Hz throughout the entire experiment. The effects of vehicle control (black squares), isoproterenol alone (1 nM; green diamonds), Ro 20-1724 alone (10 μM; black triangles) or both Ro and isoproterenol (red circles) are shown. Bars on the graph indicate the times at which either Ro 20-1724 or isoproterenol were present. Data represent the mean ± standard error of the mean for n = 7-12 experiments and are expressed relative to unloaded cell shortening at t=0 minutes. (a) indicates data significantly different ($p<0.05$) from its appropriate control. (b) indicates data significantly different ($p<0.05$) than the isoproterenol only group.

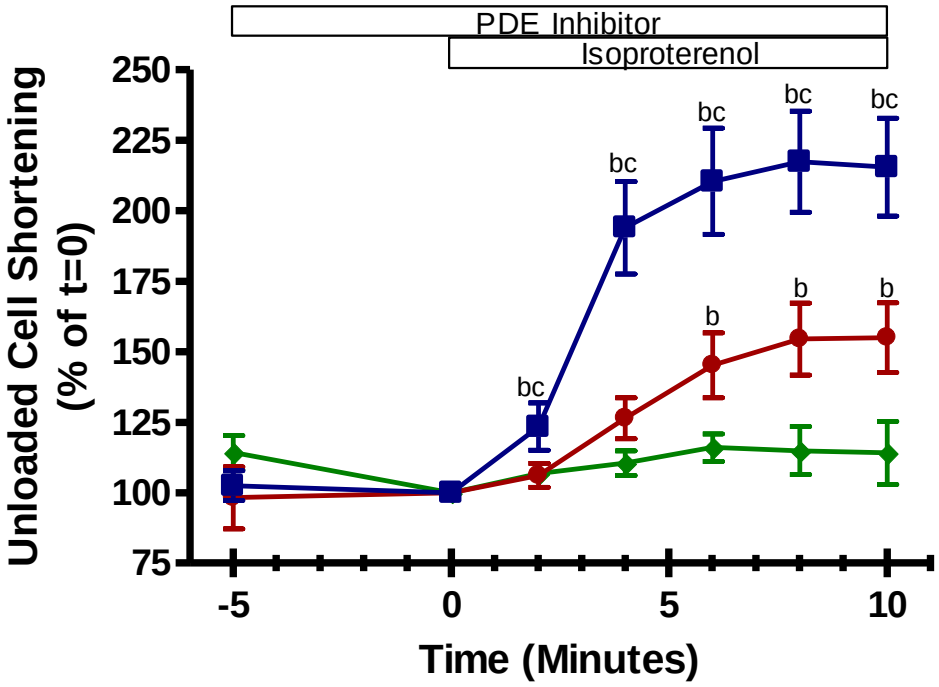

Figure 5. The effects of selective PDE3 and PDE4 inhibition on unloaded cell shortening. Cardiac myocytes were continuously field stimulated at a rate of 1Hz throughout the entire experiment. The effects of isoproterenol alone (1 nM; green diamonds), cilostamide and isoproterenol (1μM and 1 nM, respectively; blue squares) and Ro 20-1724 and isoproterenol (10μM and 1 nM, respectively; red circles) are shown. Bars on the graph indicate the times at which either a PDE inhibitor or isoproterenol were present. Data represent the mean ± standard error of the mean for n = 7-8 experiments and are expressed relative to unloaded cell shortening at t=0 minutes. (b) indicates data significantly different ($p<0.05$) than the isoproterenol only group. (c) indicates data significantly different ($p<0.05$) between the cilostamide with isoproterenol and Ro 20-1724 with isoproterenol groups.

Table 2. The Effect of PDE inhibition on Unloaded Cell Shortening

	Overload at 20 Minutes			Overload before 20 Minutes		
Treatment	None	Partial	Complete	Complete	Died	Excluded
Cilo	8					2
Ro	10					1
Cilo + Iso	6					4
Ro + Iso	7	1				1

We wished to evaluate the possible causes for this increase in unloaded cell shortening. Consequently, we decided to investigate the effects of PDE inhibition on isoproterenol-stimulated increases in $I_{Ca,L}$. Increased $I_{Ca,L}$ would cause increased calcium entry into the cell. This could directly increase cell-shortening, as well as trigger calcium induced-calcium release.

Initially, we intended to conduct the experiments using whole-cell recordings. However, in line with previous reports (Belles et al., 1988; Korn and Horn, 1989; Fukumoto et al., 2005), we found that there was a considerable decrease in the magnitude of $I_{Ca,L}$ recorded in whole cell over time. After 10 minutes of recording in the whole cell configuration, $I_{Ca,L}$ was 60 ± 8% of its magnitude at t = 0 (n = 3; Figure 6). This rundown was an indication of a loss of intracellular regulators of $I_{Ca,L}$, which caused us to conclude that this recording technique was not feasible for our experiments.

To minimize the effects of $I_{Ca,L}$ rundown, we decided to perform the experiments using the perforated patch clamp technique. In perforated patch, amphotericin B, a polyene macrolide antibiotic, is added to the pipette solution. It creates membrane spanning pores which allow for the passage of monovalent ions but does not allow dialysis of the cell and the disruption of second messenger pathways like the whole cell configuration (Korn and Horn, 1989; Liem et al., 1995). Consequently, there was no sign of rundown during control experiments using the perforated patch technique. After 10 minutes of recording in the perforated patch configuration, $I_{Ca,L}$ was 97 ± 2% of its magnitude at t = 0 (n = 8; Figure 7a). We also attempted to block the putative $I_{Ca,L}$ using 40 μM cadmium, a calcium channel blocker. We found that this concentration of

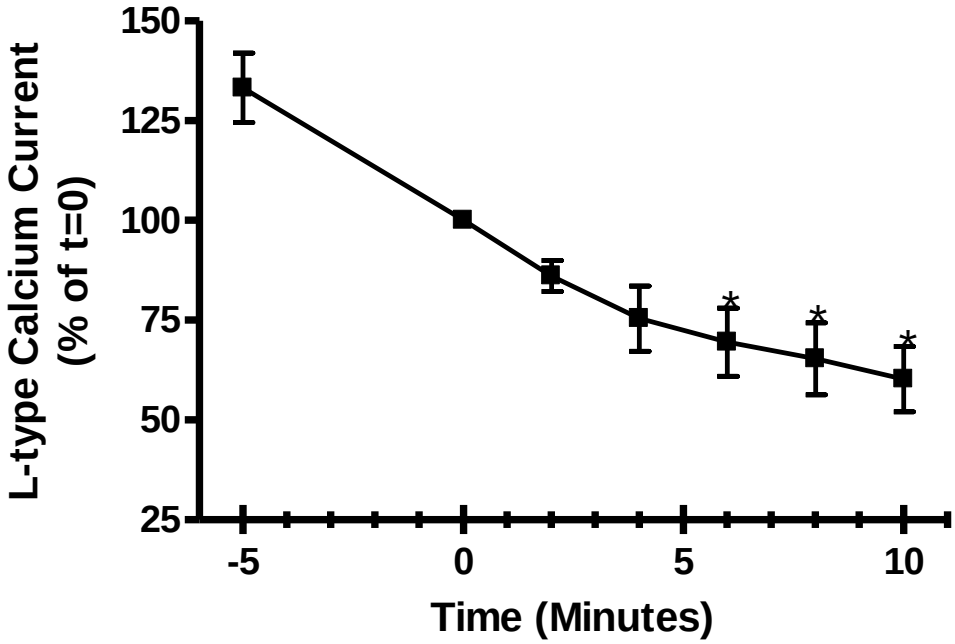

Figure 6. Rundown of calcium currents associated with the whole-cell ruptured patch technique. Cardiac myocytes were continuously stimulated in voltage-clamp to elicit calcium currents throughout the entire experiment. Data represent the mean ± standard error of the mean for n = 3 experiments and are expressed relative to calcium current at t=0 minutes. (*) indicates data significantly different from t=0 minutes.

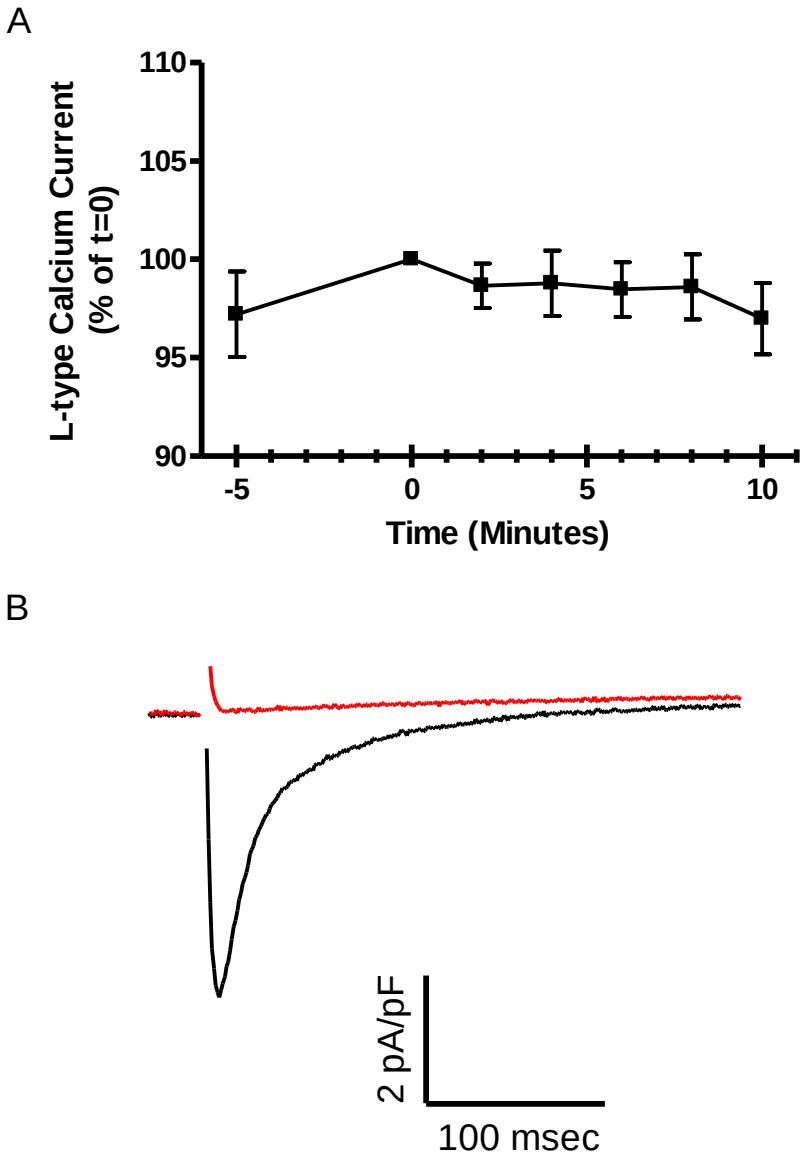

Figure 7. Calcium currents recorded using the perforated-patch technique. (A) Cardiac myocytes were continuously stimulated under voltage-clamp to elicit calcium currents throughout the entire experiment. Data represent the mean ± standard error of the mean for n = 8 experiments and are expressed relative to calcium current at t=0 minutes. (*) indicates data significantly different from t=0 minutes. (B) Representative data illustrating the effect of cadmium on perforated-patch calcium currents. Cardiac myocytes were continuously stimulated in voltage-clamp to elicit calcium currents throughout the entire experiment. The effects of cadmium (40 µM) are shown. Sample traces were recorded before (black) and 10 minutes after cadmium was administered (red). Data are representative of n = 3 experiments.

cadmium rapidly and completely blocked the currents we were recording, supporting the notion that it was, in fact, $I_{Ca,L}$ (n=3; Figure 7b).

The perforated patch recordings of $I_{Ca,L}$ used an identical format as the cell shortening experiments. For these experiments, we recorded baseline $I_{Ca,L}$ for five minutes prior to the addition of either cilostamide (1 μM), Ro 20-1724 (10 μM) or vehicle control, followed by a five minutes pre-treatment period prior to the cardiac myocytes being challenged with 1nM isoproterenol. $I_{Ca,L}$ was recorded immediately prior to the addition of isoproterenol and subsequently every two minutes over a 10 minute period. Representative data of these experiments are presented in Figure 8.

Data illustrating the effects of cilostamide pre-treatment on isoproterenol-stimulated increases of $I_{Ca,L}$ are shown in Figure 9. Addition of isoproterenol, following cilostamide pre-treatment, resulted in an increase of $I_{Ca,L}$ to 155 ± 10 % (n=6) of t=0 values at 10 minutes. This increase is significantly greater than that observed with isoproterenol alone, which was 114 ± 3 % (n=5) of t=0 values at 10 minutes. Repeating these experiments with Ro 20-1724 instead of cilostamide produced results as shown in Figure 10. In the presence of Ro 20-1724, 10 minutes exposure to isoproterenol increased $I_{Ca,L}$ to 179 ± 17 % (n=4) of t=0 values. Figure 11 is a re-plot of the cilostamide + isoproterenol and Ro 20-1724 + isoproterenol data from Figures 9 and 10. There was no significant difference between the effects of cilostamide and Ro 20-1724 following 10 minutes of isoproterenol exposure. However, there was a trend for Ro 20-1724 to have a greater effect than that observed with cilostamide.

It is important to note that many cells in the experimental groups showed signs of overload, such as spontaneous activity (Table 3). As such, it is possible that there are

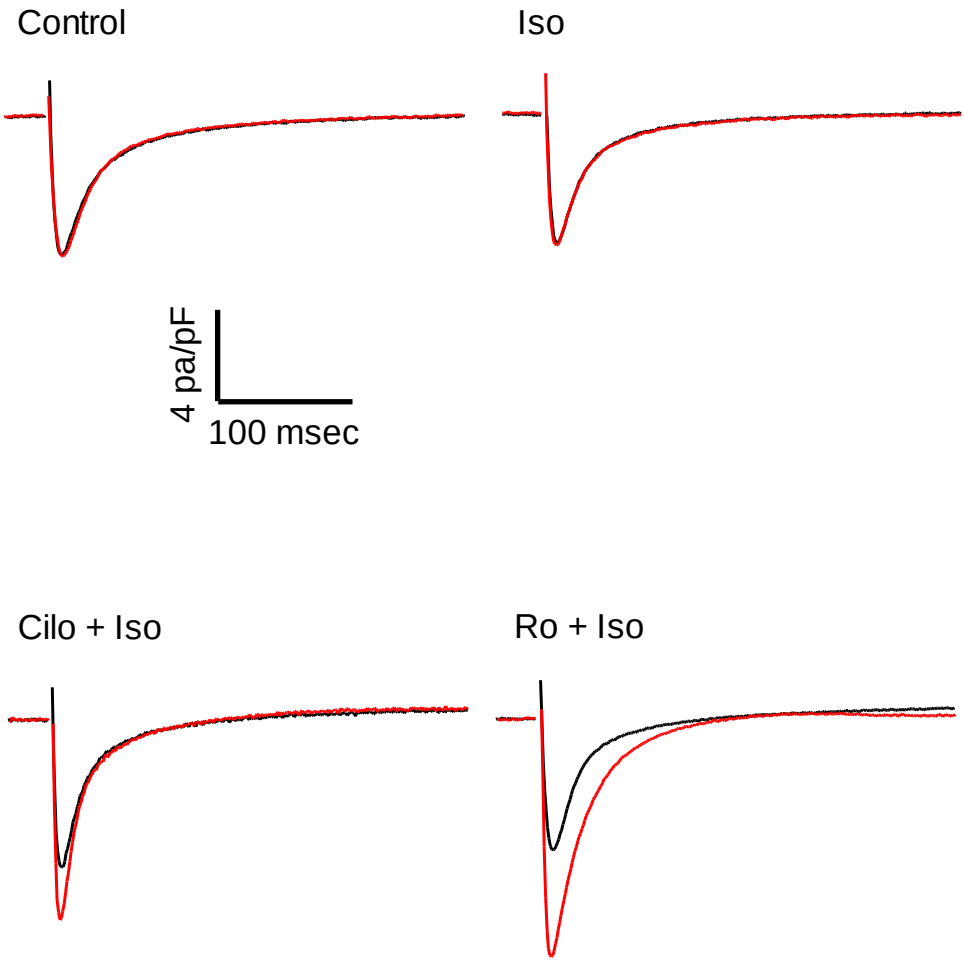

Figure 8. Representative data illustrating the effects of PDE inhibition on calcium currents. Cardiac myocytes were continuously stimulated in voltage-clamp, using perforated patch techniques, to elicit calcium currents throughout the entire experiment. The effects of vehicle control (top left), isoproterenol alone (1 nM; top right), cilostamide and isoproterenol (1μM and 1 nM, respectively; bottom left) and Ro 20-1724 + isoproterenol (10μM and 1 nM, respectively; bottom right) are shown. Baseline calcium currents were recorded for five minutes prior to the addition of PDE inhibitors, followed by a five minute pre-treatment period prior to the cardiac myocytes being challenged with isoproterenol at t=0 minutes. Calcium currents were recorded immediately prior to the addition of isoproterenol and subsequently every two minutes over a 10 minute period. Sample traces were recorded at t=0 minutes (black) and t=10 minutes (red).

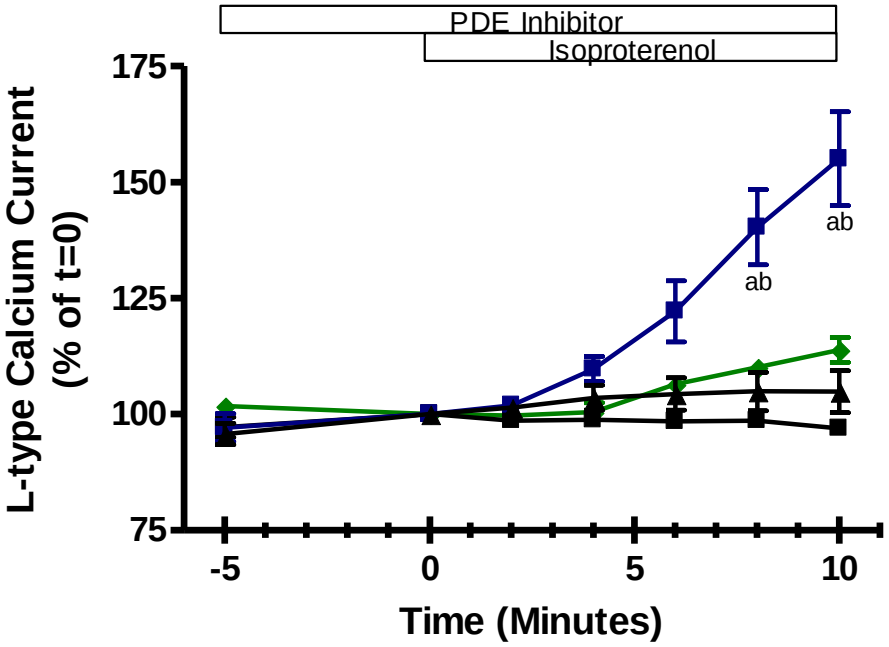

Figure 9. The effects of selective PDE3 inhibition on calcium currents. Cardiac myocytes were continuously stimulated in voltage-clamp to elicit calcium currents throughout the entire experiment. The effects of vehicle control (black squares), isoproterenol alone (1 nM; green diamonds), cilostamide alone (1 μM; black triangles) or both cilostamide and isoproterenol (blue squares) are shown. Bars on the graph indicate the times at which either cilostamide or isoproterenol were present. Data represent the mean ± standard error of the mean for n = 5-8 experiments and are expressed relative to calcium current at t=0 minutes. (a) indicates data significantly different ($p<0.05$) from its appropriate control. (b) indicates data significantly different ($p<0.05$) than the isoproterenol only group.

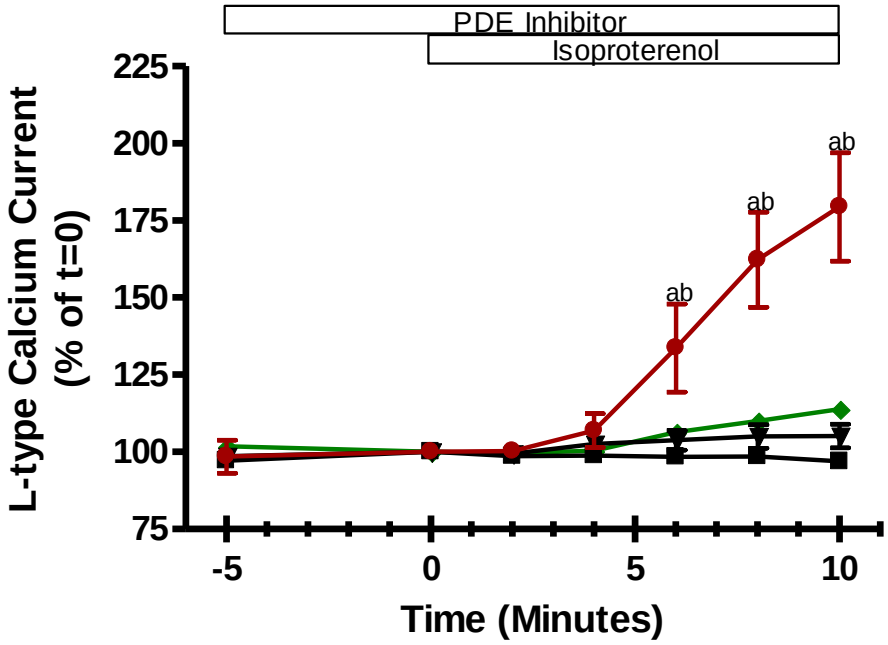

Figure 10. The effects of selective PDE4 inhibition on calcium currents. Cardiac myocytes were continuously stimulated in voltage-clamp to elicit calcium currents throughout the entire experiment. The effects of vehicle control (black squares), isoproterenol alone (1 nM; green diamonds), Ro 20-1724 alone (10 µM; black triangles) or both Ro 20-1724 and isoproterenol (red circles) are shown. Bars on the graph indicate the times at which either Ro 20-1724 or isoproterenol were present. Data represent the mean ± standard error of the mean for n = 4-8 experiments and are expressed relative to calcium current at t=0 minutes. (a) indicates data significantly different ($p<0.05$) from its appropriate control. (b) indicates data significantly different ($p<0.05$) than the isoproterenol only group.

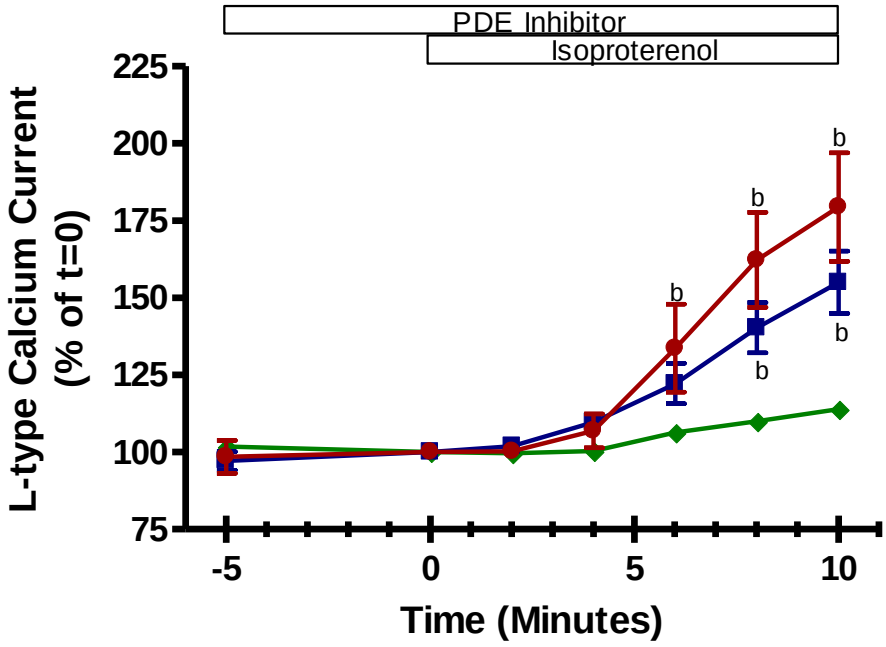

Figure 11. The effects of selective PDE3 and PDE4 inhibition on calcium currents. The effects of isoproterenol alone (1 nM; green diamonds), cilostamide and isoproterenol (1μM and 1 nM, respectively; blue squares) and Ro 20-1724 and isoproterenol (10μM and 1 nM, respectively; red circles) are shown. Bars on the graph indicate the times at which either a PDE inhibitor or isoproterenol were present. Data represent the mean ± standard error of the mean for n = 4-6 experiments and are expressed relative to unloaded cell shortening at t=0 minutes. (b) indicates data significantly different ($p<0.05$) than the isoproterenol only group.

Table 3. The Effect of PDE inhibition on Perforated Patch Calcium Currents

	Overload at 20 Minutes			Overload before 20 Minutes		
Treatment	None	Partial	Complete	Complete	Died	Excluded
Control	8				1	2
Cilo	6					4
Ro	6					2
Iso	6	5				13 *
Cilo + Iso	2	5	4			4 **
Ro + Iso		5	4		2	7 ***

* Of which four were also partially overloaded
** Of which 1 was partially overloaded
*** Of which 2 were partially overloaded

differences between these groups which are being obscured by overload. Using the same experimental design, we attempted to record $I_{Ca,L}$ in the presence of PDE inhibition and isoproterenol administration with an extracellular concentration of 0.5mM calcium as opposed to 1mM. However, 2 out of 3 cells for which we administered isoproterenol in the presence of cilostamide also went into overload.

We also tested the effects of cilostamide and Ro 20-1724 on potassium channels using the perforated patch configuration. We did this to ensure that the effects of PDE inhibition on unloaded cell shortening were not due to changes in potassium conductance. For these experiments, we recorded I_{to}, I_{K1}, I_{sus} and action potentials for five minutes prior to the addition of either cilostamide (1 μM), Ro 20-1724 (10 μM) or vehicle control. We subsequently recorded action potentials and the aforementioned potassium currents every five minutes for fifteen minutes in the presence of PDE inhibitors or vehicle control. PDE inhibition with cilostamide (n=3) or Ro 20-1724 (n=3) did not change I_{to}, I_{K1}, I_{sus} or action potentials with respect to baseline values (data not shown).

We subsequently decided to determine the effects of PDE inhibition on isoproterenol-stimulated increases in calcium transients. Calcium transients are representative of the amount of calcium influx and release from the SR per stimulation, and as such, could provide an explanation for the observed differences in unloaded cell shortening.

The calcium transient experiments used an identical format as the unloaded cell shortening and perforated patch experiments. For these experiments, we recorded baseline calcium transients for five minutes prior to the addition of either cilostamide (1μM), Ro 20-1724 (10 μM) or vehicle control, followed by a five minutes pre-treatment

period prior to the cardiac myocytes being challenged with 1nM isoproterenol. Calcium transients were recorded immediately prior to the addition of isoproterenol and subsequently every two minutes over a 10 minute period. Representative data of these experiments are presented in Figure 12.

Pooled data demonstrating the effects of cilostamide pre-treatment on isoproterenol-stimulated increases in calcium transients are shown in Figure 13. As can be seen, addition of isoproterenol, following cilostamide pre-treatment, resulted in an increase in calcium transients to 209 ± 14 % (n=8) of t=0 values at 10 minutes. This increase is significantly greater than that observed with isoproterenol alone, which was 154 ± 8 % (n=6) of t=0 values at 10 minutes. Repeating these experiments with Ro 20-1724 instead of cilostamide produced similar results, as shown in Figure 14. In the presence of Ro 20-1724, 10 minutes exposure to isoproterenol increased calcium transients to 185 ± 12 % (n=8) of t=0 values. Figure 15 is a re-plot of the cilostamide + isoproterenol and Ro 20-1724 + isoproterenol data from Figures 13 and 14. As can be seen, there was no significant difference between the effects of cilostamide and Ro 20-1724 following 10 minutes of isoproterenol exposure. However, there was a trend for the effects of cilostamide to be greater than those for Ro 20-1724.

Overload was not as prevalent in these experiments as in the perforated patch recordings (Tables 3, 4). This was probably due, at least in part, to the intracellular calcium buffering effects of fluo-3. However, because the experimental groups were slightly but not significantly different, we decided to do these recordings with an extracellular calcium concentration of 0.5mM. The experimental design was the same as

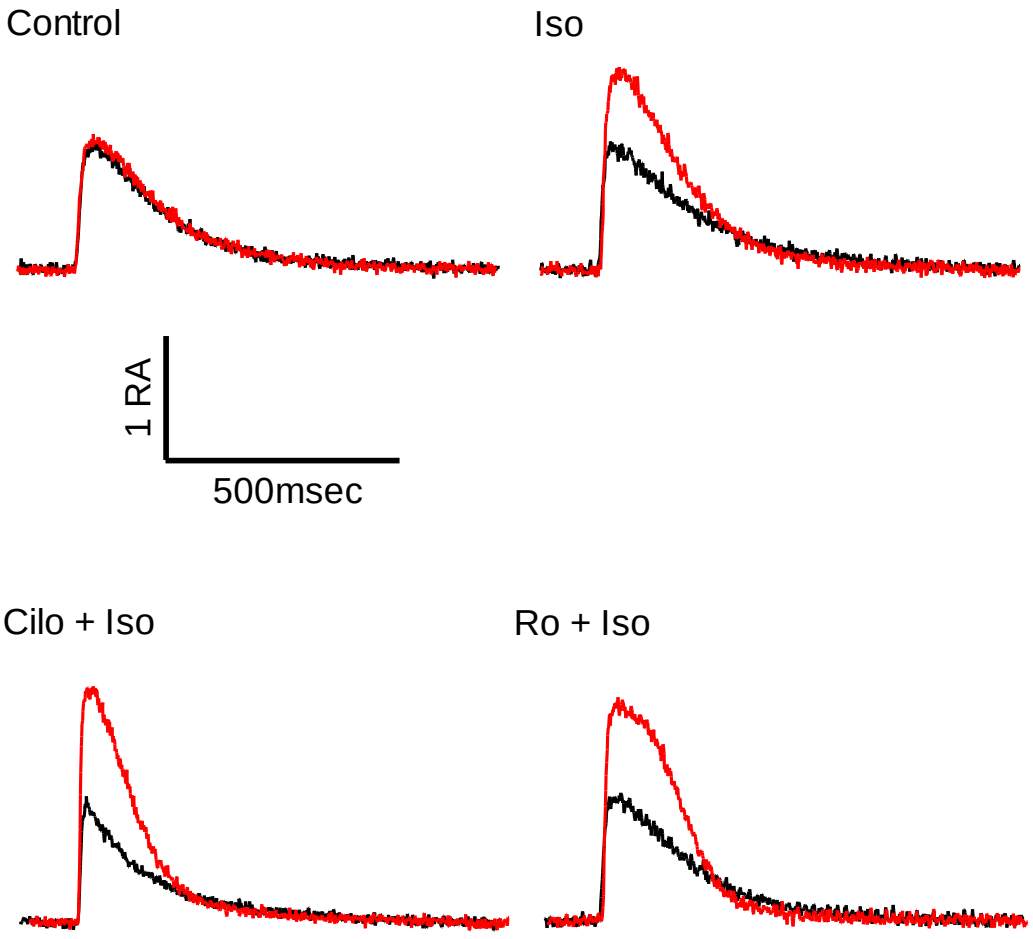

Figure 12. Representative data illustrating the effects of PDE inhibition on calcium transients. Cardiac myocytes were continuously field stimulated at a rate of 1Hz throughout the entire experiment. The effects of vehicle control (top left), isoproterenol alone (1 nM; top right), cilostamide and isoproterenol (1μM and 1 nM, respectively; bottom left) and Ro 20-1724 + isoproterenol (10μM and 1 nM, respectively; bottom right) are shown. Baseline calcium transients were recorded for five minutes prior to the addition of PDE inhibitors, followed by a five minute pre-treatment period prior to the cardiac myocytes being challenged with isoproterenol at t=0 minutes. Calcium transients were recorded immediately prior to the addition of isoproterenol and subsequently every two minutes over a 10 minute period. Sample traces were recorded at t=0 minutes (black) and t=10 minutes (red). Because the data were recorded in arbitrary units, all tracings were expressed relative to t=0, which was assigned a relative amplitude (RA) of 1.

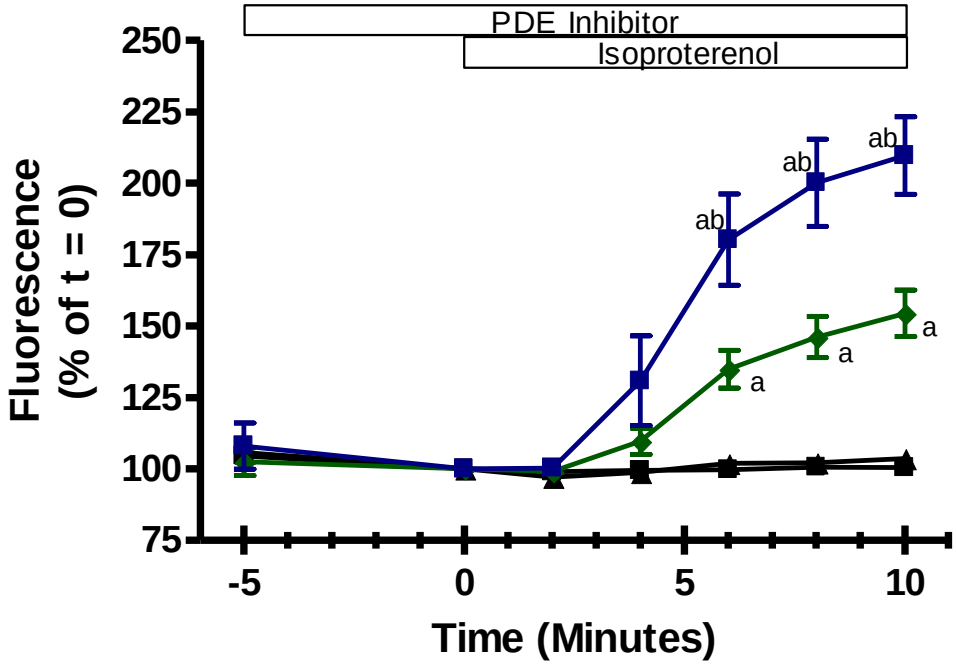

Figure 13. The effects of selective PDE3 inhibition on calcium transients. Cardiac myocytes were continuously field stimulated at a rate of 1Hz throughout the entire experiment. The effects of vehicle control (black squares), isoproterenol alone (1 nM; green diamonds), cilostamide alone (1 μM; black triangles) or both cilostamide and isoproterenol (blue squares) are shown. Bars on the graph indicate the times at which either cilostamide or isoproterenol were present. Data represent the mean ± standard error of the mean for n = 6-12 experiments and are expressed relative to calcium transient at t=0 minutes. (a) indicates data significantly different ($p<0.05$) from its appropriate control. (b) indicates data significantly different ($p<0.05$) than the isoproterenol only group.

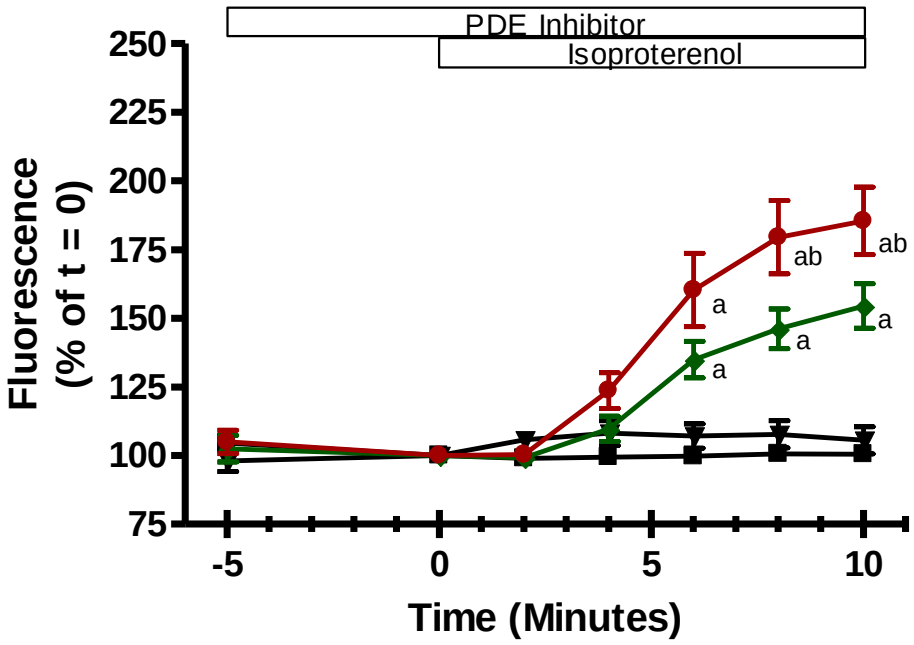

Figure 14. The effects of selective PDE4 inhibition on calcium transients. Cardiac myocytes were continuously field stimulated at a rate of 1Hz throughout the entire experiment. The effects of vehicle control (black squares), isoproterenol alone (1 nM; green diamonds), Ro 20-1724 alone (10 μM; black triangles) or both Ro 20-1724 and isoproterenol (red circles) are shown. Bars on the graph indicate the times at which either Ro 20-1724 or isoproterenol were present. Data represent the mean ± standard error of the mean for n = 6-12 experiments and are expressed relative to calcium transient at t=0 minutes. (a) indicates data significantly different ($p<0.05$) from its appropriate control. (b) indicates data significantly different ($p<0.05$) than the isoproterenol only group.

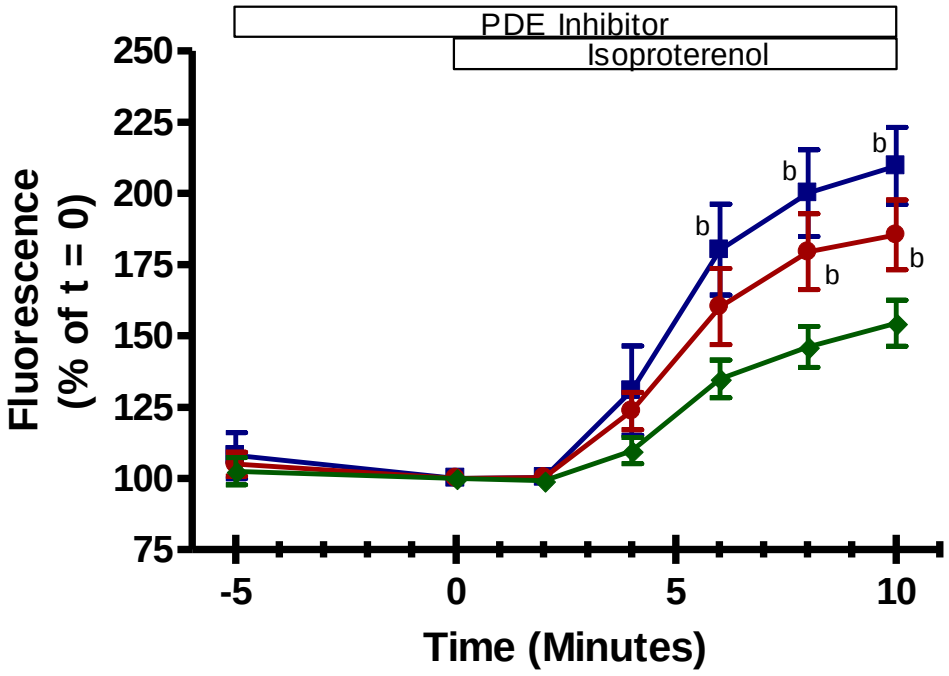

Figure 15. The effects of selective PDE3 and PDE4 inhibition on calcium transients. Cardiac myocytes were continuously field stimulated at a rate of 1Hz throughout the entire experiment. The effects of isoproterenol alone (1 nM; green diamonds), cilostamide and isoproterenol (1μM and 1 nM, respectively; blue squares) and Ro 20-1724 and isoproterenol (10μM and 1 nM, respectively; red circles) are shown. Bars on the graph indicate the times at which either a PDE inhibitor or isoproterenol were present. Data represent the mean ± standard error of the mean for n = 6-9 experiments and are expressed relative to calcium transient at t=0 minutes. (b) indicates data significantly different ($p<0.05$) than the isoproterenol only group. (c) indicates data significantly different ($p<0.05$) between the cilostamide with isoproterenol and Ro 20-1724 with isoproterenol groups.

Table 4. The Effect of PDE inhibition on Calcium Transients

	Overload at 20 Minutes			Overload before 20 Minutes		
Treatment	None	Partial	Complete	Complete	Died	Excluded
Control	12					1
Cilo	9					1
Ro	9					3
Iso	6					1
Cilo + Iso	7	1				2
Ro + Iso	6	3				2

for the previous calcium transient experiments. The addition of isoproterenol following cilostamide pre-treatment resulted in an increase in calcium transients to 224 ± 16 % of t=0 values at 10 minutes (n=7; Figure 16). This was not significantly different from the addition of isoproterenol following Ro 20-1724 pre-treatment, which resulted in an increase in calcium transients to 203 ± 16 % (n=7) of t=0 values. There was no overload present in these experiments.

We subsequently set out to discover whether or not there are differences in PDE3 and PDE4 mediated effects on calcium uptake into the sarcoplasmic reticulum following β-adrenergic stimulation. We did this by performing caffeine pulse experiments to deplete the SR of its calcium stores. In order to preserve the format of the previous experiments, we initially attempted to administer caffeine pulses at five minute intervals. However, we found that this amount of time between caffeine administration did not allow the cells to fully regain their pre-caffeine function. Consequently, we decided to switch to the administration of caffeine every ten minutes, which required slight modifications in the experimental protocol with respect to previous experiments.

For the SR calcium load experiments, we recorded baseline calcium transients for five minutes prior to the first caffeine pulse recording. We subsequently washed out the caffeine for five minutes prior to the addition of either cilostamide (1 μM), Ro 20-1724 (10 μM) or vehicle control. This was followed by a five minute pre-treatment period before the cardiac myocytes were given a second caffeine pulse. At the conclusion of the second caffeine pulse, myocytes were challenged with 1nM isoproterenol for ten minutes prior to the third caffeine pulse recording. Representative data of these experiments is presented in Figure 17.

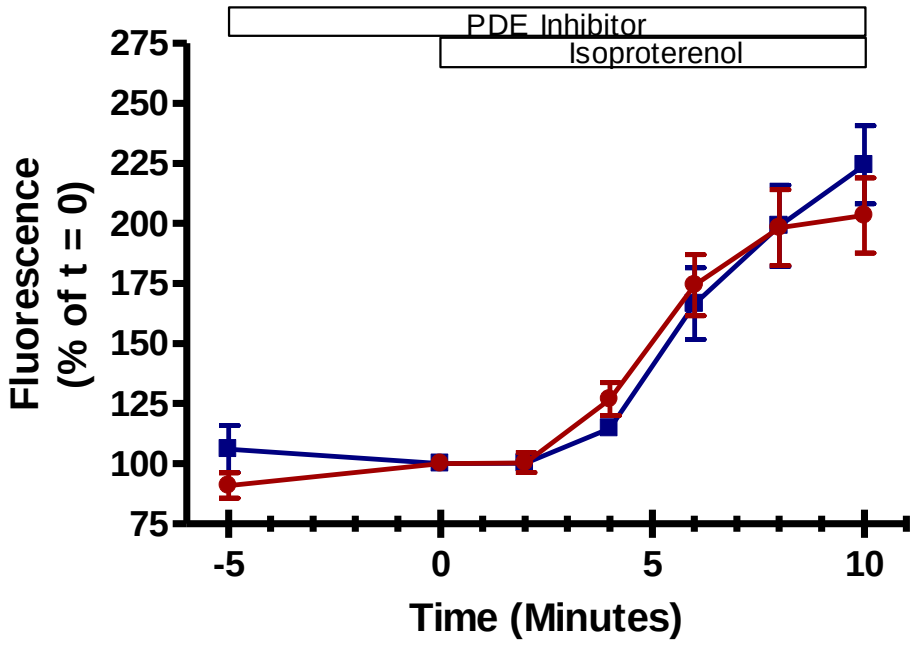

Figure 16. The effects of selective PDE3 and PDE4 inhibition on calcium transients with 0.5mM external Ca^{2+}. Cardiac myocytes were continuously field stimulated at a rate of 1Hz throughout the entire experiment. The effects of cilostamide and isoproterenol (1μM and 1 nM, respectively; blue squares) and Ro and isoproterenol (10μM and 1 nM, respectively; red circles) are shown. Bars on the graph indicate the times at which either a PDE inhibitor or isoproterenol were present. Data represent the mean ± standard error of the mean for n = 7 experiments and are expressed relative to calcium transient at t=0 minutes. (*) indicates data significantly different ($p<0.05$) between the cilostamide with isoproterenol and Ro 20-1724 with isoproterenol groups.

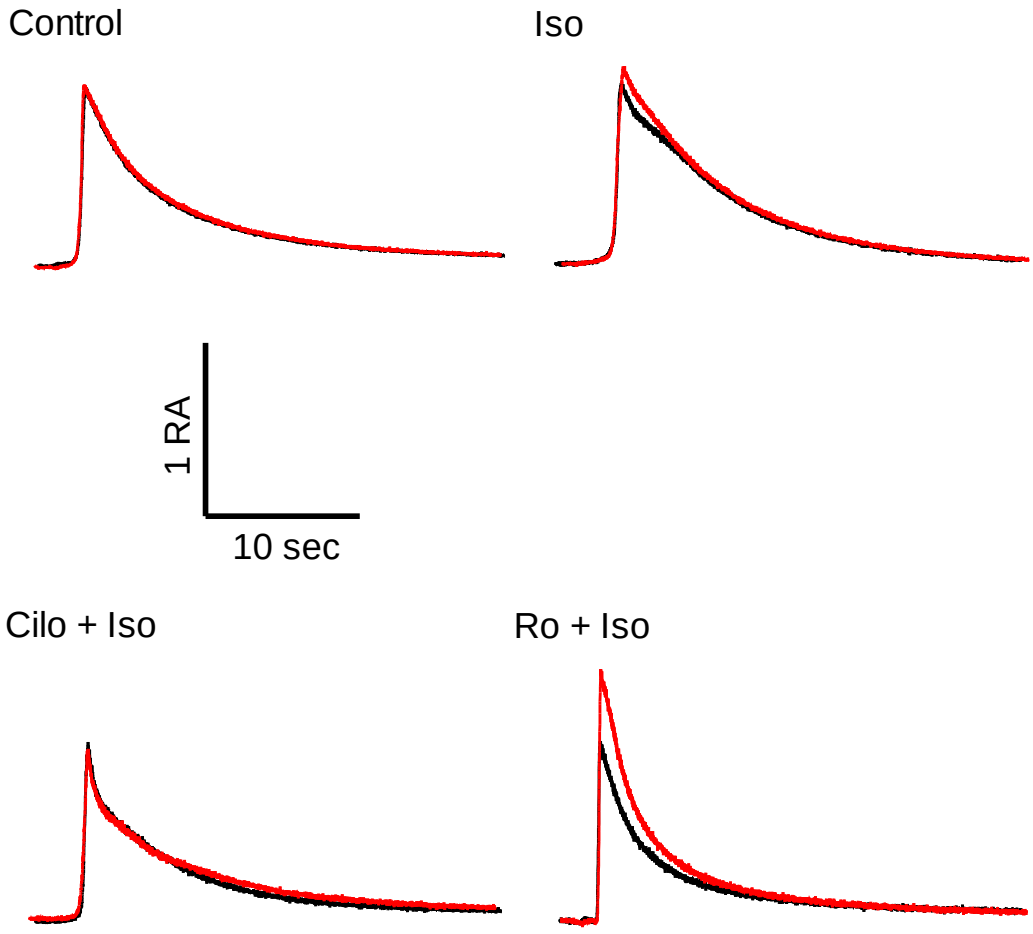

Figure 17. Representative data illustrating the effects of PDE inhibition on SR calcium load. Cardiac myocytes were continuously field stimulated at a rate of 1Hz, except during caffeine pulses. The effects of vehicle control (top left), isoproterenol alone (1 nM; top right), cilostamide and isoproterenol (1μM and 1 nM, respectively; bottom left) and Ro 20-1724 + isoproterenol (10μM and 1 nM, respectively; bottom right) are shown. Baseline calcium transients were recorded for five minutes prior to the first caffeine pulse, which was followed by five minutes of perfusion with standard Tyrode's solution. PDE inhibitors were subsequently administered for a five minute pre-treatment period prior to the cardiac myocytes being challenged with isoproterenol at t=0 minutes. Caffeine pulses were performed immediately prior to the addition of isoproterenol, and subsequently after 10 minutes of isoproterenol administration. Sample traces were recorded at t=0 minutes (black) and t=10 minutes (red). Because the data were recorded in arbitrary units, all tracings were expressed relative to t=0, which was assigned an RA of 1.

Data illustrating the effects of cilostamide pre-treatment on the impact of isoproterenol on SR calcium load are shown in Figure 18. Addition of isoproterenol, following cilostamide pre-treatment, resulted in an SR calcium load to 113 ± 9 % (n=6) of t=0 values at 10 minutes. This value for SR calcium load was not significantly different from that observed with isoproterenol alone, which was 114 ± 6 % (n=5) of t=0 values at 10 minutes. Repeating these experiments with Ro 20-1724 instead of cilostamide produced results as shown in Figure 19. In the presence of Ro 20-1724, 10 minutes exposure to isoproterenol increased SR calcium load to 139 ± 9 % (n=6) of t=0 values. Figure 20 is a re-plot of the cilostamide + isoproterenol and Ro 20-1724 + isoproterenol data from Figures 18 and 19. As can be seen when the data are presented together, the effects of Ro 20-1724 were significantly greater than those of cilostamide after 10 minutes of isoproterenol exposure. There were fairly low levels of overload in these experiments (Table 5).

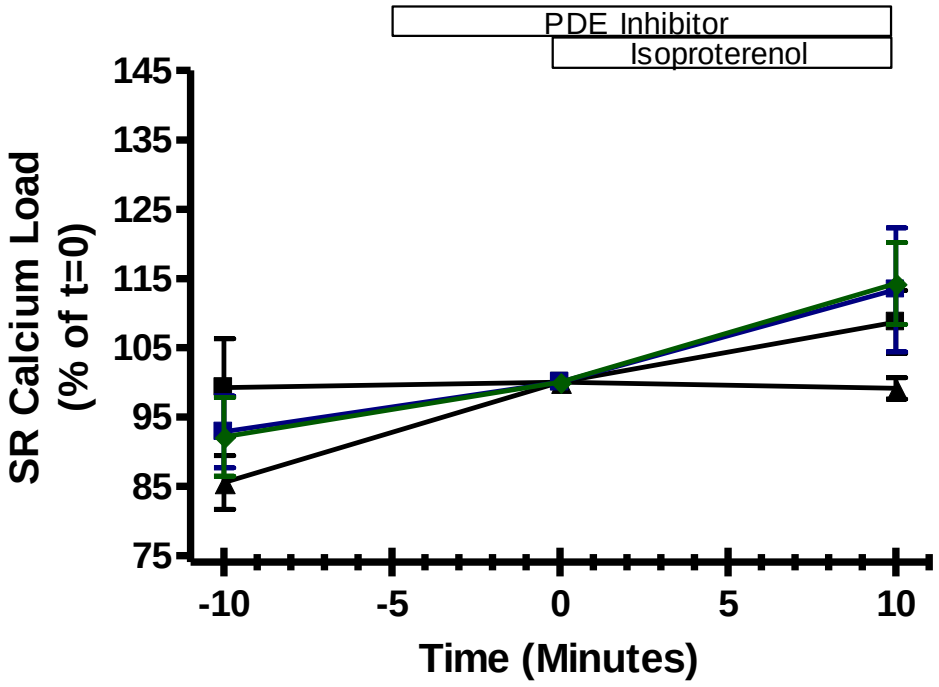

Figure 18. The effects of selective PDE3 inhibition on SR calcium load. Cardiac myocytes were continuously field stimulated at a rate of 1Hz throughout the entire experiment, except during caffeine pulses. The effects of vehicle control (black squares), isoproterenol alone (1 nM; green diamonds), cilostamide alone (1 μM; black triangles) or both cilostamide and isoproterenol (blue squares) are shown. Bars on the graph indicate the times at which either cilostamide or isoproterenol were present. Data represent the mean ± standard error of the mean for n = 5-7 experiments and are expressed relative to SR calcium load at t=0 minutes.

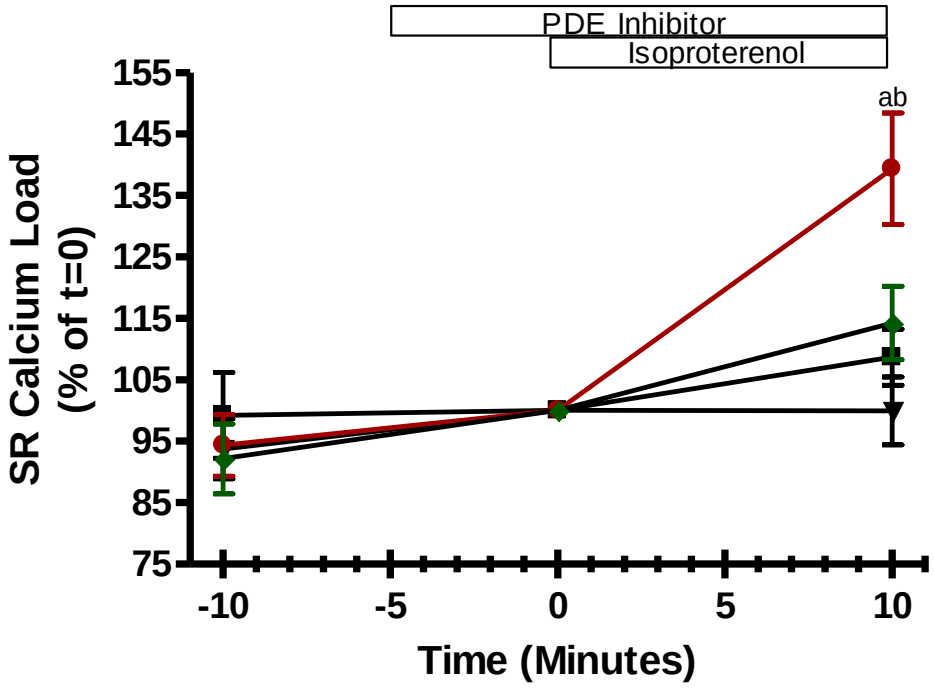

Figure 19. The effects of selective PDE4 inhibition on SR calcium load. Cardiac myocytes were continuously field stimulated at a rate of 1Hz throughout the entire experiment, except during caffeine pulses. The effects of vehicle control (black squares), isoproterenol alone (1 nM; green diamonds), Ro 20-1724 alone (10 μM; black triangles) or both Ro 20-1724 and isoproterenol (red circles) are shown. Bars on the graph indicate the times at which either Ro 20-1724 or isoproterenol were present. Data represent the mean ± standard error of the mean for n = 5-7 experiments and are expressed relative to SR calcium load at t=0 minutes. (a) indicates data significantly different ($p<0.05$) from its appropriate control. (b) indicates data significantly different ($p<0.05$) than the isoproterenol only group.

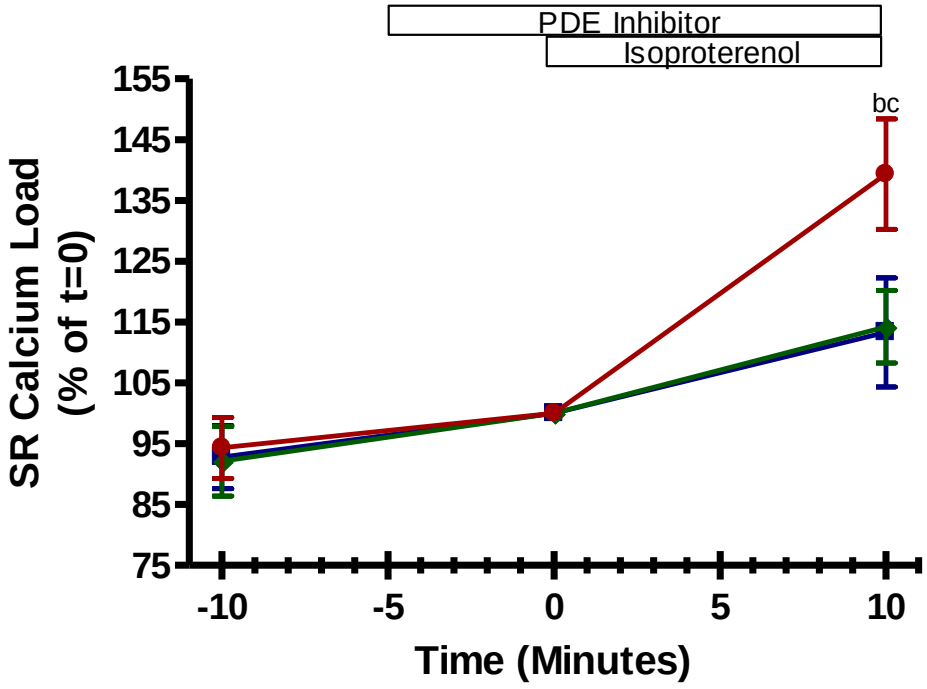

Figure 20. The effects of selective PDE3 and PDE4 inhibition on sarcoplasmic reticulum calcium load. Cardiac myocytes were continuously field stimulated at a rate of 1Hz throughout the entire experiment, except during caffeine pulses. The effects of isoproterenol alone (1 nM; green diamonds), cilostamide and isoproterenol (1μM and 1 nM, respectively; blue squares) and Ro 20-1724 and isoproterenol (10μM and 1 nM, respectively; red circles) are shown. Bars on the graph indicate the times at which either a PDE inhibitor or isoproterenol were present. Data represent the mean ± standard error of the mean for n = 5-6 experiments and are expressed relative to SR calcium load at t=0 minutes. (b) indicates data significantly different ($p<0.05$) than the isoproterenol only group. (c) indicates data significantly different ($p<0.05$) between the cilostamide with isoproterenol and Ro 20-1724 with isoproterenol groups.

Table 5. The Effect of PDE inhibition on SR Calcium Load

	Overload at 20 Minutes			Overload before 20 Minutes		
Treatment	None	Partial	Complete	Complete	Died	Excluded
Control	7				2	1
Cilo	6				3	2
Ro	6				1	1
Iso	5				2	1
Cilo + Iso	6				1	
Ro + Iso	6				4	3

CHAPTER 4: DISCUSSION AND CONCLUSIONS

Summary

This study demonstrated that isoproterenol administration, in the presence of PDE3 inhibition, resulted in a larger increase in unloaded cell shortening compared to those recorded in the presence of PDE4 inhibition. There was a trend for PDE4 inhibition and isoproterenol administration to cause a larger increase in calcium currents than PDE3 inhibition and isoproterenol administration, although this increase was not significant. There was also a trend for PDE3 inhibition to cause a larger increase in calcium currents than PDE4 inhibition with isoproterenol administration, although again, this increase was not significant. Finally, PDE4 inhibition and isoproterenol administration caused a larger increase in SR-calcium loading than PDE3 inhibition and isoproterenol administration. These results indicate that PDE3 may be localized in proximity to the contractile apparatus of cardiac myocytes, while PDE4 may be localized in a domain consisting of the L-type calcium channel and junctional SR (Figure 21). As such, our study provides functional evidence for differential localization of PDE isoforms in cardiac myocytes.

Compartmentation of PDE3 and PDE4

The results of this study would suggest that PDE4 is associated with t-tubule L-type calcium channels and the junctional SR, while PDE3 could be associated with the contractile apparatus. This is because PDE4 inhibition and isoproterenol stimulation increased SR calcium load more than PDE3 inhibition and isoproterenol stimulation, and produced a non-significant trend in the same direction for calcium currents. On the other

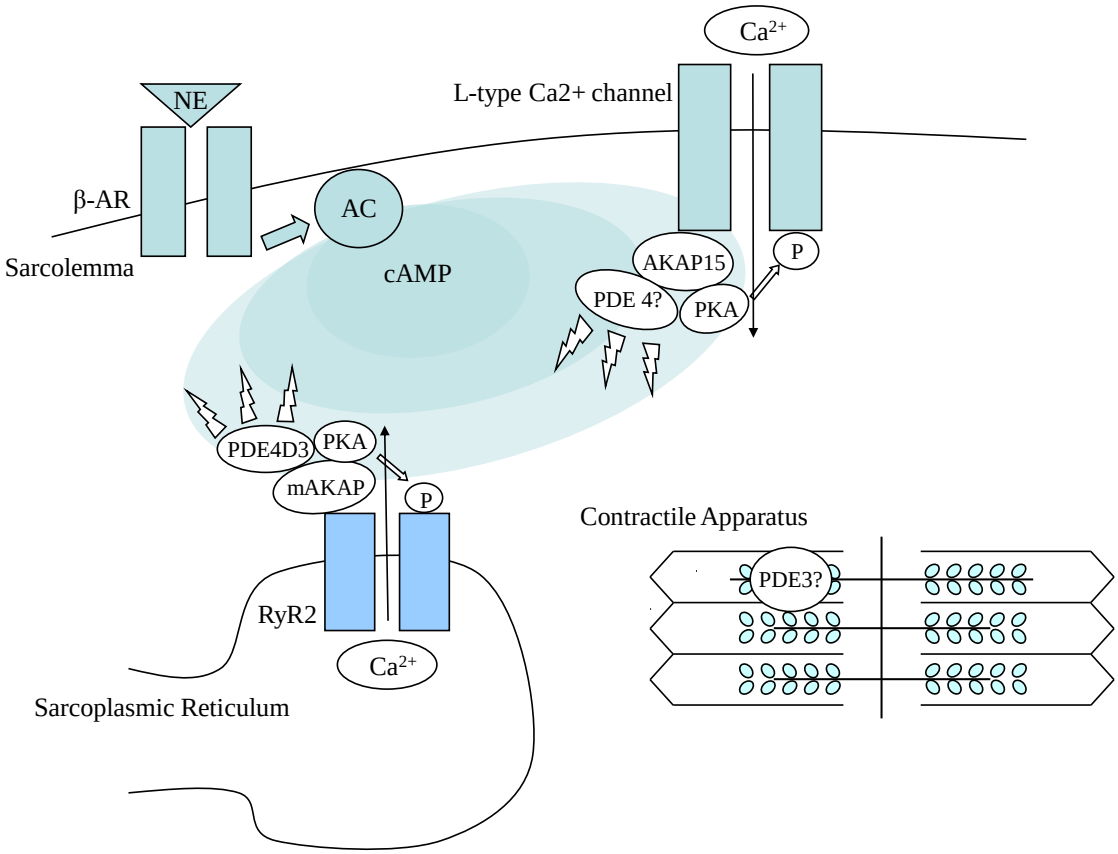

Figure 21. Conceptual model for the localization of the β-AD signaling cascade by PDEs in cardiac myocytes. The results of our study suggest the possibility of PDE3 in association with the contractile apparatus. Additionally, our results suggest that PDE4 is associated with $I_{Ca,L}$ and RyR2.

hand, PDE3 inhibition and isoproterenol stimulation increased unloaded cell shortening more than PDE4 inhibition and isoproterenol stimulation.

There is support in the literature for differential PDE3 and PDE4 localization. Mongillo et al. (2004) found that PDE3 and PDE4 were localized differently in neonatal rat cardiac myocytes; PDE3 was localized on internal membranes while PDE4 was localized to the M-line and Z-line. The t-tubule network is closely apposed to Z-lines in ventricular myocytes (Gao et al, 1997). A significant fraction of L-type Ca^{2+} channels are localized to the t-tubules in proximity to SR Ca^{2+} release channels in cardiac myocytes (Balijepalli et al. 2006). AKAP100 also co-localizes to the Z-line and transverse tubule/junctional SR region in adult rat cardiac myocytes (Yang et al, 1998). Additionally, the results of Hulme et al. (2003) indicate that PKA is bound to AKAP15, which in turn binds to $Ca_V1.2$. Consequently, it is possible that an AKAP-PDE4-PKA complex exists at the L-type calcium channel, similar to the one elucidated for RyR2 (Dodge et al., 2001; Lehnart et al., 2005). The existence of such a complex, or the established presence of PDE4 in this domain, could explain why PDE4 inhibition and β-AD stimulation resulted in larger (though non-significant) increase in calcium currents with respect to PDE3 inhibition.

Like the L-type calcium channel and RyR, key elements of the β-AD signaling cascade such as Gs and AC are concentrated at the t-tubules (Reviewed in Brette and Orchard, 2003). Using isoproterenol in the presence of PDE inhibitors, Nikolaev et al. (2006) found that cAMP generated by β-adrenergic stimulation was primarily regulated by PDE4. Perry et al. (2002) found that β-arrestins recruit PDE4D isoforms to the β_2-AR to attenuate PKA activation. Blocking PDE4 would interfere with this method of

quenching the cAMP signal, and could, in part, explain the effects of PDE4 inhibition in our study. Interestingly, Kerfant et al. (2007) found that PDE4D co-immunoprecipitated with the SR-calcium uptake pump SERCA2a. Blocking PDE4 would lessen the amount of cAMP "drained away" from SERCA2a in response to β-AD stimulation, and would cause more calcium uptake into the SR. In fact, this is what was seen in our experiments; PDE4 inhibition, but not PDE3 inhibition, resulted in an increased SR calcium load in response to β-AD stimulation.

As such, PDE4 would seem to exert its effects in the vicinity of the t-tubules and junctional sarcoplasmic reticulum. PDE3 does not seem to be as central to the regulation of cAMP generated by β-adrenergic stimulation as PDE4. Nikolaev et al. (2006) found PDE2, in fact, contributed more to hydrolysis of cAMP generated by β-AD stimulation than PDE3, with a mechanism for PDE2 activity provided by (Mongillo et al., 2006). However, PDE3 inhibition in humans with milrinone (Packer et al., 1991) and theyophylline (Bittar and Friedman, 1991) is highly deleterious, whereas there is an absence of evidence suggesting any negative cardiovascular effects of PDE4 inhibition.

Hambleton et al. (2005) set out to determine the localization of PDE3 activity in the human myocardium. They found that PDE3 comprised the major cAMP hydrolytic activity in the microsomal fraction under all conditions. However, PDE3 had a decreased role in the microsome in the presence of elevated intracellular calcium and high cAMP, characteristics of β-AD stimulation. Under these conditions, they found high levels of non-PDE3 PDE activity in the cytosol. At reduced calcium and cAMP, there was a reduced contribution from PDE1 and other PDEs in the cytosol and an increased role for PDE3 (Hambleton et al. 2005).

The results of our study indicate that PDE3 is possibly somehow associated with the contractile apparatus of adult rat ventricular myocytes. This would seem to run counter to the results of Hambleton et al. (2005), who found that PDE3 was primarily associated with the microsomal fraction under conditions which replicated β-AD stimulation, although there could be experimental or species related differences at play. The reason why our results indicate this possible association is because PDE3 inhibition and isoproterenol administration caused a larger increase in cell shortening than PDE4 inhibition and isoproterenol administration, while it had no effect on SR calcium load. This would tend to indicate that PDE3 is more associated with a contractile domain than with the t-tubule and junctional SR domain proposed for PDE4.

The question remains of why, then, PDE3 inhibition and isoproterenol stimulation affected calcium currents and calcium transients. It is possible that the increase in PDE3 inhibition and β-AD stimulation increased intracellular cAMP enough to cause spillover of cAMP from the PDE3 domain to the PDE4 domains, which PDE4 was unable to completely hydrolyze. In their 2004 study, Mongillo et al. found that β-AD stimulation, in the presence of cilostamide resulted in a transient increase in cAMP, while β-AD stimulation in the presence of Ro 20-1724 resulted in a stable increase. They explained this by saying that cAMP not metabolized under conditions of PDE3 inhibition was metabolized by PDE4. However, their studies were FRET measurements of cAMP in quiescent myocytes, not functional measurements in actively contracting cells, and it is possible that this contributed to the divergent results.

Limitations of Unloaded Cell Shortening Experiments

Calcium overload was a major factor in unloaded cell shortening and perforated patch experiments. Unloaded cell shortening recordings lasted for 10 seconds, with a stimulation frequency of 1Hz. Partial overload was defined as the presence of sub-maximal contractions as well as maximal contractions for each recording. Complete overload was defined as the absence of maximal contractions per recording. Oftentimes, cells in complete overload began to contract uncontrollably, and were no longer producing even sub-maximal contractions with the pulses. Cell death was defined in the same way for unloaded cell shortening recordings as for calcium current, calcium transient and SR calcium load recordings. Namely, cell death was defined as when cells lost their rectangular shape and curled up into a ball.

The technical reasons for excluding cells from the final data were issues across all unloaded cell shortening experimental groups. Two of the most common reasons were that the cell had almost stopped contracting by t=0 minutes, and that there was a problem with the edge detectors being able to reliably follow the cell edges. Cells were generally selected that were initially contracting in the 5 to 7% range. All cells underwent a five minute equilibration period, and a subsequent five minute period during which either vehicle control or PDE inhibitors were added before the administration of isoproterenol at t=0 minutes. During this period, some cells decreased in their contraction to 1 or 2% of their resting lengths. As such, these cells were barely contracting by the time isoproterenol was administered, and were consequently excluded from analysis. This was one of the reasons for the large number of excluded cells in the 10nM group; three of

the cells excluded for technical reasons were noted to have almost stopped contracting before drug administration.

Another common cause for excluding cells from the cell shortening data was problems with the edge detectors, a device which uses light/dark contrast to follow the edges of a cell as it contracts. The cells occasionally shifted, and this could cause the edge detector to record contractility at an odd angle or to record multiple points of contrast on the cell. Problems also arose when cells had attained maximal percent shortening. At times, the edge detectors could no longer generate complete traces, making analysis difficult. As such, cells with incomplete traces were often excluded from analysis.

Other issues arose when recording cell shortening that also presented themselves in the electrophysiology and fluorescence experiments. Problems of this nature included changes in flow rate when switching the perfusion from vehicle control to drug-treatment groups. After these instances, the flow-rate would be recalibrated, but if the flow rate had been much too slow during drug perfusion, the cell would oftentimes be excluded from analysis. However, the most pervasive issue common to all experimental types was when a dead cell near the experimental cell would shift and come in contact with the experimental cell. When this would occur, the experimental cell would be excluded from analysis.

Limitations of Calcium Current Experiments

There were two calcium current traces per 10 second recording. Partial overload was defined as when at least one maximal current was elicited per time point, if

necessary, by making multiple recordings. Maximal calcium currents were assessed by simultaneously recording unloaded cell shortening with calcium currents. Cells were defined to produce maximal calcium currents when they contracted upon stimulation, whereas cells that contracted during the voltage ramp generated smaller currents and interfered in our ability to record maximal calcium currents due to reactivation kinetics of the channels. Complete overload occurred when cells only contracted during the voltage ramp, or began fibrillating, and it became impossible to produce a single recording when they contracted on the pulse.

An explanation for the large number of excluded cells in the isoproterenol group is that we performed these recordings first and initially did not simultaneously record fractional cell shortening. Many of these cells appeared to be in mild overload, and were generating currents of slightly different sizes on different pulses. However, because we were unable to correlate a current with a contraction, we excluded these cells and redid the experiments while recording fractional cell shortening.

There were several reasons we excluded perforated patch cells. We excluded cells that were contracting during the voltage ramp before the administration of any drugs. This indicated that the cell was already in mild overload, and as such, treatments designed to increase calcium entry into the cell produced variable results. Cells that took on a blotchy appearance during the experiment and seemed to lose their striations were also excluded. This was taken to be representative of poor cell health and viability.

Furthermore, we excluded cells that stopped contracting during the experiment. Cells in the perforated patch configuration contract upon stimulation. We followed the common practice of adding EGTA to our intracellular solution to provide us with a way

to assess whether the cells had gone into the whole cell configuration during the experiment. If the cells did go whole cell, EGTA would diffuse in, chelate the intracellular calcium and prevent contraction. Finally, we excluded cells that ended the experiments with an access resistance of greater than 20 MΩ. The R_a of cells in perforated patch should decrease from 20 MΩ at the beginning of the recording to less than ten MΩ, ideally during the equilibration period before any drugs are administered. If a cell has an R_a greater than 20 MΩ at the end of the experiment, this indicated that the access resistance was increasing after the point at which it should have stabilized, usually generating currents that were artificially smaller than they should have been.

A question arises as to why the overload present in the calcium current recordings was more severe than that in the unloaded cell shortening recordings. The answer to this question is probably related to the difference in the duration of the stimulus applied to elicit either a calcium current or a contraction. For the perforated patch recordings, the cells were held in a depolarized state for 300msec, during which calcium entered into the cell and the calcium currents were recorded. In contrast, the cells were only exposed to an electrical current for 5msec to elicit contraction in the unloaded cell shortening recordings. Consequently, increases in the amount of calcium entry into the cells due to drug treatment were more likely to cause overload in the perforated patch recordings with respect to the unloaded cell shortening recordings. This is due to the fact that a great deal more calcium was entering the cells in the perforated patch recordings to begin with.

Limitations of Calcium Transient and SR Calcium Loading Experiments

Calcium transient recordings lasted for 10 seconds, with a stimulation frequency of 1Hz. SR calcium load recordings lasted for 75 or 90 seconds, with a stimulation frequency of 1Hz to elicit calcium transients prior to the administration of caffeine. A possible explanation for the comparative lack of overload in these experiments is that the fluorescent indicators used for these experiments, either fluo-3 for calcium transients, or fluo-4 for caffeine pulses, chelates intracellular calcium. Consequently, the presence of these fluorescent dyes buffered the large increases in intracellular calcium present with PDE inhibition and β-AD stimulation. This would also suggest a method whereby we could eliminate the significant overload featured in the unloaded cell shortening, and especially calcium current experiments.

As with the other experiments, there were technical reasons that lead to the exclusion of calcium transient and caffeine pulse data from the results. Sometimes, bubbles from the oil would move into the field of the microscope, changing the diffraction of light and magnitude of fluorescence. On one occasion, the stimulator moved, causing a shadow to develop over the cell. As in other experiments, dead cells would sometimes shift to touch the experimental cell. Finally, the buffer perfusion system would occasionally sweep cells off the plate. For the caffeine pulse experiments, this would make sense given the rapid solution exchange and gravity-limited flow of the caffeine containing buffer onto the plate. However, this also occurred for calcium transient experiments. In total, the incidence of technical problems was much less for the fluorescence experiments than for the unloaded cell shortening, and especially the

calcium current experiments. This can probably be at least partially attributed to the negligible overload present in these cells due to intracellular calcium buffering by the fluorescent dyes.

Comparison to Previous Studies

Previous investigations have used similar approaches to explore the concept of PDE compartmentation (Rochais et al., 2006; Kerfant et al., 2007). Both of these studies report findings that are both consistent and inconsistent with our study, which may be partially explained by the experimental limitations discussed. It is possible to question the necessity of our experiments given a paper recently published by Rochais et al. (2006). They performed experiments testing the effects of cilostamide and Ro 20-1724 on $I_{Ca,L}$ in the presence of the β-adrenergic agonist isoprenaline. These experiments seem to be similar to the ones which we have proposed, but there are important differences.

Rochais et al. (2006) performed whole cell experiments in cultured myocytes to examine the effects of cilostamide and Ro 20-1724 on $I_{Ca,L}$ in the presence of the β-adrenergic agonist isoprenaline. In comparison to our study, important differences are the rundown of $I_{Ca,L}$ during the control period evident in their recordings and the use of adult ventricular myocytes subjected to tissue culture conditions for a 24 hour period rather than freshly isolated myocytes. The latter is important because studies have shown that changes in electrophysiological properties of cardiac myocytes can occur after a single day in culture (Reviewed in Mitcheson et al., 1998). Additionally, Rochais et al. performed their experiments by adding cilostamide in the presence of isoprenaline, washing it out, and then adding Ro 20-1724 to the same cell. This introduces numerous

confounding variables, including the possibility of incomplete wash-out. We performed our experiments by testing the effects of cilostamide and Ro-20 1724 on $I_{Ca,L}$ in different cells. Finally, Rocahis et al. (2006) did not study the effect of β-adrenergic stimulation on contractility, calcium transients and SR calcium load in the presence of PDE3 and PDE4 inhibition.

The results of our experiments are different than those found by Kerfant et al. (2007). The focus of their study was on the effects of PI3Kγ knockout on $I_{Ca,L}$, calcium transients and SR calcium load in the presence and absence of PDE3 and PDE4 inhibition. PI3Kγ acts as a kinase which can alter cardiac contractility and ECC through its regulations of basal cAMP levels and phospholamban phosphorylation. PI3Kγ has been found to stimulate PDE3B, and consequently may exert some of its effects through the activation of PDEs to hydrolyze cAMP.

The work of Kerfant et al. (2007) is relevant because of discrepancies between their control experiments and the control experiments of this study. They found PDE3 inhibition with milrinone or PDE4 inhibition with rolipram did not affect $I_{Ca,L}$, but increased calcium transients and SR calcium content in left ventricular mouse myocytes. These effects were present in the absence of a cAMP generating agonist such as isoproterenol. Although no effects were evident on $I_{Ca,L}$, it is important to note that these experimenters employed the whole cell patch technique. As previously mentioned, this does not seem to be an optimal way to study second messenger microdomains, as whole cell causes dialysis of the cellular contents by the pipette solution (Liem et al., 1995). For example, Liem et al. (1995) specifically recommend using perforated patch to study forskolin activation of cAMP in order to leave the intracellular machinery intact. In

addition, calcium current rundown in whole cell is well-known (Belles et al., 1988; Korn and Horn, 1989; Fukumoto et al., 2005) and was experienced in our study, although none was evident in the work of Kerfant et al. (2007).

Kerfant et al. (2007) also used very different methodologies than the current study for measuring calcium transients and SR calcium load, both of which relied on whole cell patch clamping. They recorded calcium transients simultaneously with $I_{Ca,L}$ by adding 0.05mM fluo-3 to the pipette solution. Kerfant et al. (2007) estimated SR calcium load by performing whole cell recordings of sodium-calcium exchange currents (I_{NCX}) in response to 20mM caffeine. It is possible that the use of electrophysiology to measure calcium transients and to estimate SR calcium load allowed Kerfant et al. (2007) to record changes in response to PDE inhibition even in the absence of exogenous cAMP stimulation. However, the increases they observed are fairly prominent, and we found no effect of PDE inhibition in the absence of isoproterenol stimulation when recording unloaded cell shortening, calcium currents, calcium transients and SR calcium load. Additionally, as previously mentioned, the use of whole cell electrophysiology to study second messenger microdomains is problematic.

Future directions

One of the largest problems encountered in this study was calcium overload of actively contracting myocytes. This was probably a most significant problem for the perforated patch calcium current recordings. Reducing the external calcium concentration from 1mM to 0.5mM did not seem to remedy this problem. Even at this calcium concentration, two out of three cells for which we administered isoproterenol in

the presence of cilostamide went into overload. However, two other options are available; to perform the experiments with barium as the charge carrier (Thu et al., 2006), or to use fluo-3 or fluo-4 to buffer intracellular calcium. The second option presented itself upon the observation that there was very little calcium overload during the fluorescence experiments (Tables 4, 5). Performing these experiments without overload would enable us to better elucidate differences in PDE3 and PDE4 inhibition on calcium currents.

It would also be useful to determine the effects of mAKAP disruption on the aforementioned parameters using either mAKAP inhbitors or siRNA techniques. mAKAPs have been shown to physically anchor PDE4 to RyR2 (Dodge et al., 2001; Lehnart et al., 2005), and it would be interesting to investigate if their disruption attenuates the effects of selective PDE inhibition. Finally, hormones other than catecholamines result in the production of cAMP, including glucagon and prostaglandin E_1 (Rochais et al., 2006). According to the compartmentation theory, different PDEs should be involved in the regulation of distinct pools of cAMP produced in response to specific hormones. As such, it is possible that PDE control over the cAMP produced in response to these agonists is different from that controlling cAMP generated by β-AD stimulation.

Conclusions

It is exciting to think that differential phosphodiesterase localization contributes to a widely conserved second messenger, cAMP, producing a highly specific signal. Additionally, disruption of PDE localization can be demonstrated to have dramatic consequences in living cells. The results of this study represent an opportunity and a challenge to those attempting to explore phosphodiesterase inhibition for its potential clinical applications. The opportunity stems from the fact that disruption of these pathways has profound functional effects which could ideally be employed for a therapeutic benefit. However, this opportunity also presents a challenge. Disruption of PDE regulation of cAMP has been shown to have deleterious effects evident from the level of the single cell to the entire organism. As such, phosphodiesterases represent an important therapeutic target, so long as we find ways to alter finely tuned cAMP pathways without producing cellular chaos.

REFERENCES

Balijepalli RC, Foell JD, Hall DD, Hell JW, Kamp TJ. (2006). Localization of cardiac L-type Ca(2+) channels to a caveolar macromolecular signaling complex is required for beta(2)-adrenergic regulation. *Proceedings of the National Academy of Sciences* **103**, 7500-5.

Beavo JA, Brunton LL. (2002). Cyclic nucleotide research -- still expanding after half a century. *Nature Reviews Molecular Cellular Biology* **3**, 710-8.

Belles B, Malecot CO, Hescheler J, Trautwein W. (1988). "Run-down" of the Ca current during long whole-cell recordings in guinea pig heart cells: role of phosphorylation and intracellular calcium. Pflugers Archiv. *European Journal of Physiology* **411**, 353-60.

Bittar G, Friedman HS. (1991). The arrhythmogenicity of theophylline. A multivariate analysis of clinical determinants. *Chest* **99**, 1415-20.

Brette F, Leroy J, Le Guennec JY, Sallé L. (2005). Ca^{2+} currents in cardiac myocytes: Old stories, new insights. *Progress in Biophysics and Molecular Biology* **91**, 1-82. Review.

Brette F, Orchard C. (2003) T-tubule function in mammalian cardiac myocytes. *Circulation Research* **92**, 1182-92. Review.

Brillantes AMB, Ondrias K, Scott A, Kobrinsky E, Ondriasova E, Moschella MC, Jayaraman T, Landers M, Ehrlich BE, Marks AR. (1994). Stabilization of calcium release channel (ryanodine receptor) function by FK506-binding protein. *Cell* **77**, 513-23.

Dodge KL, Khouangsathiene S, Kapiloff MS, Mouton R, Hill EV, Houslay MD, Langeberg LK, Scott JD. (2001). mAKAP assembles a protein kinase A/PDE4 phosphodiesterase cAMP signaling module. *The European Molecular Biology Organization Journal* **20**, 1921-30.

Fukumoto GH, Lamp ST, Motter C, Bridge JH, Garfinkel A, Goldhaber JI. (2005). Metabolic inhibition alters subcellular calcium release patterns in rat ventricular myocytes: implications for defective excitation-contraction coupling during cardiac ischemia and failure. *Circulation Research* **18**, 551-57.

Gao T, Puri TS, Gerhardstein BL, Chien AJ, Green RD, Hosey MM. (1997). Identification and subcellular localization of the subunits of L-type calcium channels and adenylyl cyclase in cardiac myocytes. *Journal of Biological Chemistry* **272**, 19401-7.

Gee KR, Brown KA, Chen WN, Bishop-Stewart J, Gray D, Johnson I. (2000). Chemical and physiological characterization of fluo-4 Ca^{2+}-indicator dyes. *Cell Calcium* **27**, 97-106.

Hambleton R, Krall J, Tikishvili E, Honeggar M, Ahmad F, Manganiello VC, Movsesian MA. (2005). Isoforms of cyclic nucleotide phosphodiesterase PDE3 and their contribution to cAMP hydrolytic activity in subcellular fractions of human myocardium. *Journal of Biological Chemistry* **280**, 39168-74.

Hendrickson WA. (2005). Transduction of biochemical signals across cell membranes. *Quarterly Reviews of Biophysics* **38**, 321-30

Hulme JT, Lin TWC, Westenbroek RE, Scheuer T, Catterall WA. B-adrenergic regulation requires direct anchoring of PKA to cardiac $Ca_V1.2$ channels via a leucine zipper interaction with a kinase-anchoring protein 15. *Proceedings of the National Academy of Sciences of the USA* **100**, 13093-98.

Iacovelli L, Sallese M, Mariggio S, de Blasi A. (1999). Regulation of G-protein-coupled receptor kinase subtypes by calcium sensor proteins. *FASEB Journal* **13**, 1-8. Review.

Insel PA, Head BP, Ostrom RS, Patel HH, Swaney JS, Tang CM, Roth DM. (2005). Caveolae and lipid rafts: G protein-coupled receptor signaling microdomains in cardiac myocytes. *Annals of the New York Academy of Sciences* **1047**, 166-72. Review.

Jurevicius J and Fischmeister R. (1996). cAMP compartmentalization is responsible for a local activation of cardiac Ca^{2+} channels by β-adrenergic agonists. *Proceedings of the National Academy of Sciences of the USA* **93**, 295-99.

Kerfant BG, Zhao D, Lorenzen-Schmidt I, Wilson LS, Cai S, Chen SR, Maurice DH, Backx PH. (2007). PI3Kgamma is required for PDE4, not PDE3, activity in subcellular microdomains containing the sarcoplasmic reticular calcium ATPase in cardiomyocytes. *Circulation Research* **101**, 400-8.

Korn SJ and Horn R. (1989) Influence of sodium-calcium exchange on calcium current rundown and the duration of calcium-dependent chloride currents in pituitary cells, studied with whole cell and perforated patch recording. *Journal of General Physiology* **94**, 789–812

Krebs EG and Beavo JA. (1979). Phosphorylation-dephosphorylation of enzymes. Annual *Review of Biochemistry* **48**, 923-59.

Kohout TA, Lin FS, Perry SJ, Conner DA, Lefkowitz RJ. (2001). beta-Arrestin 1 and 2 differentially regulate heptahelical receptor signaling and trafficking. *Proceedings of the National Academy of Sciences* **98**, 1601-6.

Langan TA. (1968). Histone phosphorylation: stimulation by adenosine 3',5'-monophosphate. *Science* **162**, 579-580.

Laflamme MA and Becker PL. (1999) Gs and adenylyl cyclase in transverse tubules of the heart: implications for cAMP-dependent signaling. *American Journal of Physiology – Heart and Circulatory Physiology* **277**, 1841-48.

Lehnart SE, Wehrens XHT, Reiken S, Warrier S, Belevych AE, Harvey RD, Richter W, Jin SLC, Conti M, Marks AR. (2005). Phosphodiesterase 4D deficiency in the ryanodine-receptor complex promotes heart failure and arrhythmias. *Cell* **123**, 25-35.

Liem LK, Simard JM, Song Y, Tewari K. (1995). The patch clamp technique. *Neurosurgery* **36**, 382-92. Review.

Lohmann SM, Walter U, Greengard P. (1980). Identification of endogenous substrate proteins for cAMP-dependent protein kinase in bovine brain. *Journal of Biological Chemistry* **255**, 9985-92.

Maier LS, Bers DM. (2007). Role of Ca2+/calmodulin-dependent protein kinase (CaMK) in excitation-contraction coupling in the heart. *Cardiovascular Research* **73**, 631-40. Review.

Marx S, Reiken S, Hisamatsu Y, Jayaraman T, Burkhoff D, Rosemblit N, Marks AR. (2000). PKA phosphorylation dissociates FKBP12.6 from the calcium release channel (ryanodine receptor): defective regulation in failing hearts *Cell* **101**, 365-76.

Mitcheson JS, Hancox JC, Levi AJ. 1998. Cultured adult cardiac myocytes: future applications, culture methods, morphological and electrophysiological properties. *Cardiovascular Research* **39**, 280-300. Review.

Mongillo M, McSorley T, Evellin S, Sood A, Lissandron V, Terrin A, Huston E, Hannawacker A, Lohse MJ, Pozzan T, Houslay MD, Zaccolo M. (2004). Fluorescence resonance energy transfer-based analysis of cAMP dynamics in live neonatal rat cardiac myocytes reveals distinct functions of compartmentalized phosphodiesterases. *Circulation Research* **95**, 67-75.

Mongillo M, Tocchetti CG, Terrin A, Lissandron V, Cheung YF, Dostmann WR, Pozzan T, Kass DA, Paolocci N, Houslay MD, Zaccolo M. (2006). Compartmentalized phosphodiesterase-2 activity blunts beta-adrenergic cardiac inotropy via an NO/cGMP-dependent pathway. *Circulation Research* **98**, 226-34.

Mongillo M, Zaccolo M. (2006). A complex phosphodiesterase system controls beta-adrenoceptor signalling in cardiomyocytes. *Biochemical Society Transactions* **34**, 510-11. Review.

Nagendran J, Archer SL, Soliman D, Gurtu V, Moudgil R, Haromy A, St Aubin C, Webster L, Rebeyka IM, Ross DB, Light PE, Dyck JR, Michelakis ED. (2007). Phosphodiesterase type 5 is highly expressed in the hypertrophied human right ventricle,

and acute inhibition of phosphodiesterase type 5 improves contractility. *Circulation* **116**, 238-48.

Nikolaev VO, Bunemann M, Schmitteckert E, Lohse MJ, Engelhardt S. (2006) Cyclic AMP imaging in adult cardiac myocytes reveals far-reaching beta1-adrenergic but locally confined beta2-adrenergic receptor-mediated signaling. *Circulation Research* **99**, 1084-91.

Ono K, Fozzard HA. (1992). Phosphorylation restores activity of L-type calcium channels after rundown in inside-out patches from rabbit cardiac cells. *The Journal of Physiology* **454**, 673-88.

Oude Weernink PA, Han L, Jakobs KH, Schmidt M. (2007). Dynamic phospholipid signaling by G protein-coupled receptors. *Biochimica et Biophysica Acta* **1768**, 888-900. Review.

Packer M, Carver JR, Rodeheffer RJ, Ivanhoe RJ, Dibianco R, Zeldis SM, Hendrix GH, Bommer WJ, Elkayam U, Kukin ML, Mallis GI, Sollano JA, Shannon J, Tandon PK, DeMets DL. (1991). Effect of Oral Milrinone on Mortality in Sever Chronic Heart Failure. *The New England Journal of Medicine* **325**, 1468-75.

Perry SJ, Baillie GS, Kohout TA, McPhee I, Magiera MM, Ang KL, Miller WE, McLean AJ, Conti M, Houslay MD, Lefkowitz RJ. (2002). Targeting of cyclic AMP degradation to beta 2-adrenergic receptors by beta-arrestins. *Science* **298**, 834-36.

Rall TW, Sutherland EW, Wosilait WD. (1956). The relationship of epinephrine and glucagons to liver phosphorylase. III. Reactivation of liver phosphorylase in slices and in extracts. *Journal of Biological Chemistry* **218**, 483-495.

Rochais F, Abi-Gerges A, Horner K, Lefebvre F, Cooper DMF, Conti M, Fischmeister R and Vandecasteele G. (2006). A specific pattern of phosphodiesterases controls the cAMP signals generated by different G_s – coupled receptors in adult rat ventricular myocytes. *Circulation Research* **98**, 1081-88.

Rybin VO, Xu X, Lisanti MP, Steinberg SF. (2000). Differential targeting of beta -adrenergic receptor subtypes and adenylyl cyclase to cardiomyocyte caveolae. A mechanism to functionally regulate the cAMP signaling pathway. *Journal of Biological Chemistry* **275**, 41447-57.

Su Z, Li F, Spitzer KW, Yao A, Ritter M, Barry WH. (2003). Comparison of sarcoplasmic reticulum Ca2+-ATPase function in human, dog, rabbit, and mouse ventricular myocytes. *Journal of Molecular and Cellular Cardiology* **35**, 761-767.

Thu le T, Ahn JR, Woo SH. (2006). Inhibition of L-type Ca2+ channel by mitochondrial Na+-Ca2+ exchange inhibitor CGP-37157 in rat atrial myocytes. *European Journal of Pharmacology* **552**, 15-9.

Ward CA and Giles WR. (1997). Ionic mechanism of the effects of hydrogen peroxide in rat ventricular myocytes. *Journal of Physiology* **500**, 631-42.

Yang J, Drazba JA, Ferguson DG, Bond M. (1998) A-kinase anchoring protein 100 (AKAP100) is localized in multiple subcellular compartments in the adult rat heart. *Journal of Cell Biology* **142**, 511-22.

Wehrens XH, Lehnart SE, Huang F, Vest JA, Reiken SR, Mohler PJ, Sun J, Guatimosim S, Song LS, Rosemblit N, D'Armiento JM, Napolitano C, Memmi M, Priori SG, Lederer WJ, Marks AR. (2003). FKBP12.6 deficiency and defective calcium release channel (ryanodine receptor) function linked to exercise-induced sudden cardiac death. *Cell* **113**, 829-40.

Zaccolo M, Di Benedetto G, Lissandron V, Mancuso L, Terrin A, Zamparo I. (2006). Restricted diffusion of a freely diffusible second messenger: mechanisms underlying compartmentalized cAMP signalling. *Biochemical Society Transactions* **34**, 495-97. Review.

Zaccolo M, Movsesian MA. (2007). cAMP and cGMP signaling cross-talk: role of phosphodiesterases and implications for cardiac pathophysiology. *Circulation Research* **100**, 1569-78. Review.

Zaccolo M and Pozzan T. (2002). Discrete microdomains with high concentration of cAMP in stimulated rat neonatal cardiac myocytes. *Science* **295**, 1711-15.